

坦桑尼亚西南部乌本迪带内 Nsamyia 镁铁-超镁铁质杂岩体的锆石 U-Pb 年龄、地球化学特征及构造意义

许康康^{1,2)}, 刘晓阳^{1,2)}, 孙凯^{1,2)}, 龚鹏辉^{1,2)}, 吴兴源^{1,2)}, 何胜飞^{1,2)}, 孙宏伟^{1,2)}

1) 中国地质调查局天津地质调查中心, 天津, 300170; 2) 中国地质调查局华北科技创新中心, 天津, 300170

内容提要:在坦桑尼亚西南部的乌本迪带内首次发现了阿拉斯加型(岛弧型)镁铁-超镁铁环状杂岩体,对约束区域构造演化历史具有重要的意义。Nsamyia 杂岩体主要岩性为单辉橄榄岩和辉长岩,单辉橄榄岩位于杂岩体的中部,而辉长岩主要位于北部边缘,表现出环状岩体特征。锆石 U-Pb 年龄表明杂岩体的形成年龄介于 1874~1944Ma 之间,为古元古代晚期。岩石地球化学显示,杂岩体具有低 SiO₂,高 MgO、FeO_T、Cr 和 Ni 含量,富集 LREE 和 Ba、Pb、U 等大离子亲石元素,不同程度的亏损 HREE 和 Nb、Ta、Zr、Hf 和 Ti 等高场强元素特征,为具有岛弧构造背景的阿拉斯加型岩体。综合区域地质背景资料,认为其形成于古元古代乌本迪造山作用晚期的岛弧盆地闭合阶段,玄武质岩浆来源于受俯冲流体交代的岩石圈地幔,并在上升过程中遭受下地壳基底的混染作用。

关键词: Nsamyia 杂岩体; 锆石定年; 地球化学; 阿拉斯加型; 乌本迪带

造山带中出露有多种多样的镁铁-超镁铁质岩体,这些镁铁-超镁铁质岩体通常赋存有大规模的 Fe、V、Ni、Cu、Ti 和 PGE 矿床,具有重要的经济意义(Zhou Meifu et al., 2004, 2005; Feng Yanqing et al., 2017; Jiao Jiangang et al., 2017; Qin Kezhang et al., 2018)。根据镁铁-超镁铁质岩体的构造背景、岩石组合等特征,可以将其分为 5 类:蛇绿岩、义敦型岩体、阿拉斯加型岩体、层状侵入体和橄榄岩-闪长岩型岩体(Zhang Qi, 2014)。其中,阿拉斯加型镁铁-超镁铁质杂岩体是地球演化历史过程中具有规则几何形状、特殊组成和独特地质动力学意义的岩石类型(Taylor, 1967; Irvine, 1974; Himmelberg et al., 1995; Helmy et al., 2003; Eyuboglu et al., 2010; Guillou-Frottier et al., 2014),在新太古代到新生代的板块汇聚边缘都有文献记录,通常代表了长期俯冲作用相关的弧岩浆作用产物(Irvine, 1974; Himmelberg et al., 1995; Ishiwatari et al., 2004; Helmy et al., 2003; Helmy et al., 2014; Pettigrew et al., 2006; Burg

et al., 2009; Eyuboglu et al., 2010; Cai Keda et al., 2012; Sappin et al., 2012; Su Benxun et al., 2012; Guillou-Frottier et al., 2014; Tessalina et al., 2016)或弧根杂岩体(Debari et al., 1989; Batanova et al., 2005; Eyuboglu et al., 2010),因此,该类型岩体对于研究大陆岩浆弧系统内地幔源演化和监测古板块边缘地球动力学机制具有重要的意义(KePezhinskas et al., 1997; Meibom et al., 2002; Zhou Meifu et al., 2005; Polat et al., 2011; Dong Jinlong et al., 2018)。

本次在乌本迪带内首次发现了阿拉斯加型镁铁-超镁铁质岩体。乌本迪带为坦桑尼亚西南部一条重要的活动带,由 McConnell(1950)和 Sutton et al. (1954)最早发现并报道。早期许多学者认为乌本迪带的形成可分为两个阶段:前期 2100~2025Ma 的俯冲造山作用及相关的麻粒岩相变质作用,形成一系列 E-W 或 WNW-ESE 向构造组构;后期 1.9~1.8Ga 的右旋剪切作用及角闪岩相-绿片岩相变质作用叠加,形成 NW-SE 向剪切带(Daly,

注:本文为中国地质调查局项目(编号 DD20190439+121201006000150014+1212011220910)和商务部援外项目“援赞比亚东北地区航空物探和地质地球化学综合填图”[2015]352)资助的成果。

收稿日期:2020-07-06; 改回日期:2020-08-19; 网络发表日期:2020-11-20; 责任编辑:黄敏。

作者简介:许康康,男,1986年生,工程师,主要从事地质矿产勘查与研究工作。Email: xukang06@163.com.

引用本文:许康康, 刘晓阳, 孙凯, 龚鹏辉, 吴兴源, 何胜飞, 孙宏伟. 2021. 坦桑尼亚西南部乌本迪带内 Nsamyia 镁铁-超镁铁质杂岩体的锆石 U-Pb 年龄、地球化学特征及构造意义. 地质学报, 95(4):1174~1190, doi: 10.19762/j.cnki.dizhixuebao.2021028. Xu Kangkang, Liu Xiaoyang, Sun Kai, Gong Penghui, Wu Xingyuan, He Shengfei, Sun Hongwei. 2021. Zircon U-Pb age, geochemistry and tectonic significance of the Nsamyia mafic-ultramafic complex in the Ubendian Belt, southwestern Tanzania. Acta Geologica Sinica, 95(4):1174~1190.

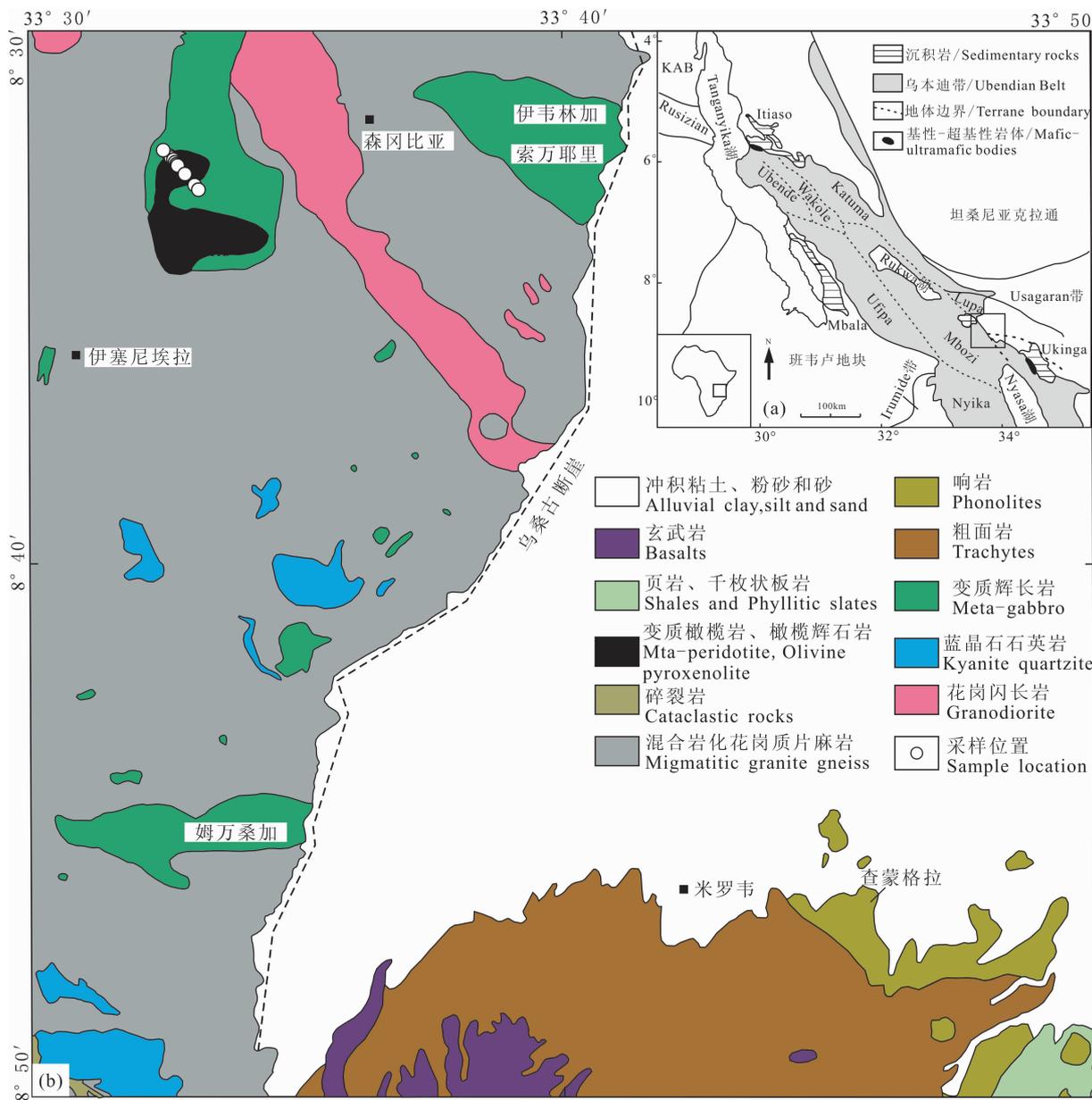


图 1 坦桑尼亚西南部乌本迪带内 Nsamyia 镁铁-超镁铁质杂岩体地质简图(据 Teale et al. , 1962)

Fig. 1 Geological sketched map of Nsamyia mafic-ultramafic complex in Ubendian Belt, southwestern Tanzania (modified after Teale et al. , 1962)

1988; Lenoir et al. , 1994; Sun Hongwei et al. , 2018). Boniface et al. (2012) 研究发现乌本迪带内发育有 $1866 \pm 14\text{Ma}$ 的榴辉岩相岩石, 并认为该带后期也经历了板块俯冲作用。然而, 有关该时期岩浆作用的研究多集中在花岗质岩石, 而以镁铁-超镁铁岩为对象的幔源岩浆活动研究相对薄弱, 从而在一定程度上限制了对区域岩浆作用与构造演化的整体认识, 造成缺乏板块俯冲作用期间幔源岩浆活动特征、幔源岩石成因及深部地质作用等过程的认识, 新发现的 Nsamyia 镁铁-超镁铁杂岩体为解决上述

问题提供了一个重要窗口。本次试图通过对该杂岩体的岩石学、年代学和地球化学等特征的系统研究, 以期探讨 Nsamyia 镁铁-超镁铁质杂岩体的源区性质和岩石成因, 为乌本迪带古元古代时期的板块构造背景认识提供一些新的依据。

1 区域地质背景

乌本迪带位于坦桑尼亚西南部, 走向 NW-SE, 长约 500km, 宽约 150km。大地构造位置上主要位于太古宙坦桑尼亚克拉通和古元古代班韦卢地块之

间,东南部为古元古代的乌萨加蓝带(Usagaran Belt),其内发育的~2.0Ga的榴辉岩相岩石代表了该地区古元古代最早期的板块俯冲活动(Möller et al., 1995),部分学者认为乌萨加蓝时期的构造运动对乌本迪带同样具有重要的影响,主要体现在两带内都存在一系列的E-W和WNW-ESE向构造组构,并认为在该时期两构造带为同一构造带(Daly, 1988; Lenoir et al., 1994)。

乌本迪带内主要岩性为麻粒岩相-绿片岩相的火山、沉积变质岩(表1)。基于不同的构造和岩石

单元,Daly et al. (1985)和Daly(1988)将乌本迪带分为8个地质体,分别命名为Ubende、Wakole、Katuma、Ufipa、Mbozi、Lupa、Upagwa和Nyika地体(图1a),不同的构造块体之间以断层或韧性剪切带接触,内部多发育NW-SE向延伸的面理,其面理的形成可能受右旋剪切作用的控制(Sutton et al., 1959; Theunissen et al., 1992),沿韧性剪切带发育有一系列的沉积盆地,如北部的Itiaso和Mbala盆地、南部的Ukingan和Mbeya盆地,构成NW-SE向拉长的狭窄构造。

表1 坦桑尼亚西南部乌本迪带地质体特征(据Daly, 1988; Boniface et al., 2017)

Table 1 Geological characteristics of the Ubendian terranes in southwestern Tanzania (modified after Daly, 1988; Boniface et al., 2017)

地体名称	地质年龄(Ma)		岩性	线理走向
	岩浆作用	变质作用		
Ubende		1890~1860Ma(榴辉岩 U-Pb 锆石)	角闪岩、榴辉岩、片麻岩和变质基性岩	ENE-WSW
		1170Ma(变质泥岩 U-Th-Pb 独居石)		
		600Ma(变质泥岩 U-Th-Pb 独居石)		
Wakole		1170~1000Ma(变质泥岩 U-Pb 锆石)	富铝硅酸岩质片岩	NW-SE
Katuma	2650Ma(变质基性岩 U-Pb 锆石)	1960Ma(变质泥岩 U-Th-Pb 独居石)	变质基性岩	NW-SE
		1940Ma(变质泥岩 U-Th-Pb 独居石)		
Ufipa	1847±37Ma(花岗岩 U-Pb 锆石)	590~520Ma(榴辉岩 U-Pb 锆石)	花岗质片麻岩	NW-SE
	1864±32Ma(花岗岩 U-Pb 锆石)			
Mbozi	2084±8Ma(片麻岩 U-Pb 锆石)		片麻岩、混合岩、石英岩±麻粒岩±变质基性岩	NW-SE
Lupa	2760Ma(花岗岩 U-Pb 金红石)		变质火山岩、花岗岩和花岗质片麻岩	NW-SE
	1943±32Ma (玄武质安山岩 U-Pb 锆石)			
	1878±15Ma(花岗岩 U-Pb 锆石)			
Upangwa	2084±86Ma(花岗岩 U-Pb 锆石)	1045±25 Ma(片麻岩 U-Pb 锆石)	变质斜长岩	NW-SE
	1880~1850Ma (石英闪长岩 U-Pb 锆石)			
	724±6Ma(花岗岩 U-Pb 锆石)			
Nyika	1990~1930Ma (花岗岩 U-Pb 锆石)	1813±13Ma; 947±7Ma; 560±6Ma (变质泥岩 U-Th-Pb 独居石)	堇青石麻粒岩	E-W
	1010±22Ma(榴辉岩 U-Pb 锆石)	1930~1969Ma(变质泥岩 Pb-Pb 锆石)		

2 岩体特征

乌本迪带内镁铁-超镁铁质杂岩体在Usangu断崖处以Nsamya杂岩体、伊韦林加-索万耶里(Lwerianga-Sowanyeri)和姆万桑加(Mwansanga)变质辉长岩体和其他的小型露头为代表,沿断崖呈线性排列特征,主要侵入到古元古代混合岩化的花岗质片麻岩中(图1b)。其中,Nsamya出露面积最大,呈南宽北窄的蝌蚪状展布,南北长约9km,东西最宽处约5km,面积约25km²。据坦桑尼亚大比例尺地质图可知,Nsamya镁铁-超镁铁质杂岩体岩性包括:变质橄榄岩、二辉橄榄岩、辉石岩、橄长岩、橄辉长岩和辉长岩,不同岩性之间未划分出明确的

地质界线。超镁铁质岩石主要局限在Nsamya Hills附近且多发生蛇纹石化,向北部延伸为变质辉长岩,呈近环状分布。坦桑尼亚地质调查局完成的1:12.5万区域地质调查结果显示,基性-超基性岩体通常穿透(penetrate)周边地质体,具有侵入来源性质,后期又遭受低级区域变质作用(Teale et al., 1962)。

根据野外观察和样品镜下薄片鉴定,结合岩石化学分析结果,确定本次采集到的Nsamya镁铁-超镁铁质杂岩体主要为单辉橄榄岩和辉长岩。其岩相学特征如下:

单辉橄榄岩:呈暗绿色-黑色,半自形粒状结构,堆晶结构,块状构造;橄榄石含量45%~55%,多蛇

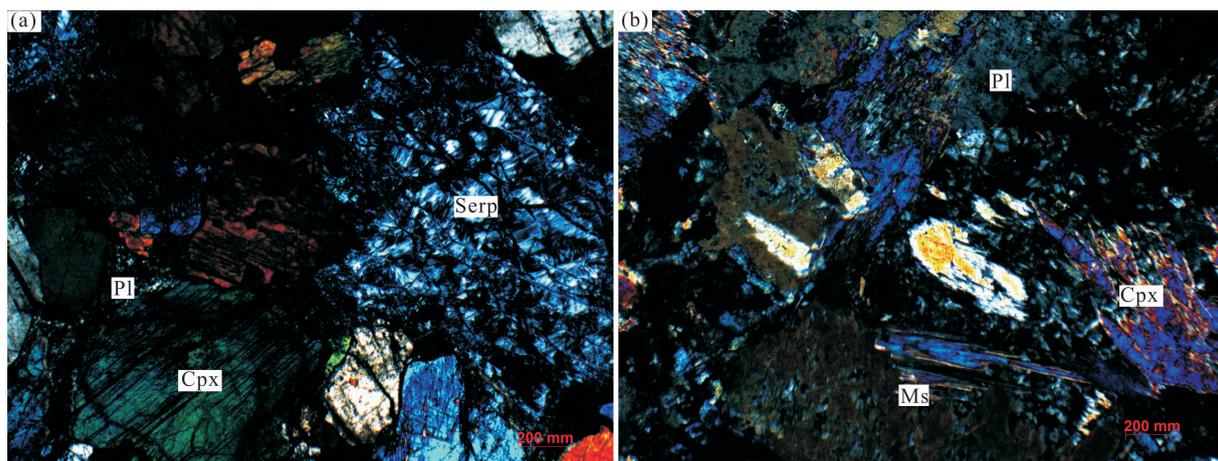


图 2 坦桑尼亚西南部 Nsamyia 杂岩体岩石镜下特征

Fig. 2 Photomicrographs from the Nsamyia complex in southwestern Tanzania

(a) 单辉橄榄岩(+);(b) 辉长岩(+);Serp—蛇纹石;Cpx—单斜辉石;Pl—斜长石;Ms—云母

(a)—Clinopyroxene peridotite; (b)—gabbro; Serp—serpentine; Cpx—clinopyroxene; Pl—plagioclase; Bi—biotite

纹石化(图 2a),发生强烈的铁质析出,常沿橄榄石裂纹或矿物边缘形成磁铁矿、铬铁矿等矿物;辉石含量为 40%~50%,为单斜辉石,斜消光,呈长板状或不规则状,多发生绿泥石化、透闪石化;斜方辉石少见,含量<5%。主要出露于岩体的中南部地区。

辉长岩:主要矿物为基性斜长石和辉石(图 2b),少量云母,副矿物包括磁铁矿、钛铁矿等;辉石含量占 30%~50%,主要为单斜辉石,多发生绿泥石化、透闪石化蚀变作用;斜长石占 45%~65%,呈半自形板状,多发生绿泥石化、绢云母化蚀变作用;云母主要为白云母,解理明显,含量 5%左右。主要出露在岩体的北部地区。

3 分析方法

3.1 锆石 U-Pb 同位素定年

锆石分选在河北省廊坊市区域地质调查研究所完成,采用常规粉碎、浮选和电磁选方法进行分选,制靶、阴极发光显微照相、透射光及反射光照相工作在北京铅年领航科技有限公司完成。锆石 U-Pb 同位素测年在天津地质调查中心实验室利用 LA-MC-ICP-MS 方法测定,所用仪器为 Thermo Fisher 公司制造的 Neptune 多接收电感耦合等离子体质谱仪及与之配套的 New wave UP 193 nm 激光剥蚀系统。利用 193 nm FX 激光器对锆石进行剥蚀,激光剥蚀的斑束为 35 μm ,激光剥蚀样品的深度为 20~40 μm 。锆石年龄计算采用国际标准锆石 91500 作为外标,元素含量采用人工合成硅酸盐玻璃 NIST SRM610 作为外标,29Si 作为内标元素进行校正。

数据处理采用 ICP MS Data Cal 程序(Liu Hongsheng et al., 2008, 2010)和 Isoplot 程序(Ludwig, 2003)进行加权平均年龄计算。

3.2 主微量元素分析

岩石地球化学样品粉碎(200 目)在河北省廊坊市宇能岩矿公司加工完成。主量元素、稀土元素及微量元素测试分析均在中国地质调查局天津地质调查中心实验室完成。主量元素采用 X 射线荧光光谱仪(XRF)测定,FeO 采用氢氟酸、硫酸溶样、重铬酸钾滴定容量法,分析精度优于 2%。稀土元素和微量元素采用电感耦合等离子体质谱仪(TJA-PQExCell ICP-MS)测定,分析精度优于 5%。

4 测试结果

4.1 锆石 U-Pb 年代学

单辉橄榄岩测年样品的中心点坐标为 E33.54°,S8.54°,其锆石 U-Pb 同位素结果列于表 2。岩体中的锆石可以分为三种:I 类型锆石共 1 颗,为半自形结构,粒径约 80 μm ,阴极发光(CL)图像(图 3a)显示,锆石为灰黑色,具有溶蚀的港湾状结构,边缘发育灰白色的变质边,具有典型的岩浆振荡环带,锆石的 U 含量为 152×10^{-6} ,Th 含量为 223×10^{-6} ,Th/U 比值为 1.47,具有岩浆锆石特征(Belousova et al., 2002)。其 $^{207}\text{Pb}/^{206}\text{Pb}$ 年龄为 $2627 \pm 19\text{Ma}$,可能代表了岩浆上升过程中捕获的围岩锆石年龄。II 类型锆石共 5 颗,多为椭圆状,粒径 60~100 μm ,阴极发光(CL)图像显示,锆石为灰色或灰黑色,边缘发育狭窄的灰白色变质边,弱分带或

面状分带,不具有岩浆振荡环带,锆石的 U 含量为 $76 \times 10^{-6} \sim 988 \times 10^{-6}$, Th 含量为 $8 \times 10^{-6} \sim 193 \times 10^{-6}$, Th/U 比值为 $0.10 \sim 0.18$, 具有变质锆石特征。5 个点的加权平均 $^{207}\text{Pb}/^{206}\text{Pb}$ 年龄为 $1874 \pm 19\text{Ma}$ (MSWD=0.23) (图 3c), 代表了岩体的变质年龄。III 类型锆石较多, 多为自形结构, 粒径 $80 \sim 130 \mu\text{m}$, 阴极发光 (CL) 图像显示, 锆石为灰色, 发育窄的岩浆振荡环带, 为典型的花岗质锆石特征, 且其 Th/U 比值通常 > 0.4 , 其 $^{206}\text{Pb}/^{238}\text{U}$ 年龄分布于 $261 \sim 682\text{Ma}$, 一颗最大 $^{207}\text{Pb}/^{206}\text{Pb}$ 年龄为 $2035 \pm 20\text{Ma}$, 这些锆石可能为后期来自花岗岩的熔体或流体携带的锆石通过微细脉渗透到岩体中, 后期的演化使得这些脉体闭合且很难在岩石中找到证据 (Shen Tingting et al., 2017), 因此不具有地质意义。

本次测得单辉橄榄岩的变质作用年龄为 $1874 \pm 19\text{Ma}$, 而其侵入的混合岩化花岗质片麻岩围岩的年龄为 $1944 \pm 10\text{Ma}$ (未发表), 因此, 推测该岩体的年龄位于 $1874 \sim 1944\text{Ma}$ 之间。另外, 在辉长岩 (18Tch02-10) 中发现一颗近椭圆形锆石 (图 3a), 阴极发光 (CL) 图像可见较宽的岩浆振荡环带, 且 Th/U 比值为 1.19 , 其 $^{207}\text{Pb}/^{206}\text{Pb}$ 年龄为 $1885 \pm 21\text{Ma}$, 可能代表了 Nsamya 岩体中辉长岩的形成年龄。超基性岩由于岩石的特殊性而不易生长锆石, 而且研究发现很多超基性岩中的锆石年龄很分散 (图 3b), 从老到新的年龄都存在, 不易确定年龄的地质意义 (Shen Tingting et al., 2017; Liu Fulai et al., 2011), 因此, 在后续的工作中还需要进一步研究确认。

表 2 坦桑尼亚西南部乌本迪带内 Nsamya 岩体的 LA-MC-ICP-MS 锆石 U-Pb 测年数据

Table 2 LA-MC-ICP-MS Zircons U-Pb isotopic data from Nsamya complex in the Ubendian Belt in southwestern Tanzania

样品 编号	元素含量 ($\times 10^{-6}$)			Th/ U	同位素比值						年龄 (Ma)					
	Pb	U	Th		$^{206}\text{Pb}/^{238}\text{U}$		$^{207}\text{Pb}/^{235}\text{U}$		$^{207}\text{Pb}/^{206}\text{Pb}$		$^{206}\text{Pb}/^{238}\text{U}$		$^{207}\text{Pb}/^{235}\text{U}$		$^{207}\text{Pb}/^{206}\text{Pb}$	
					1σ	1σ	1σ	1σ	1σ	1σ	1σ	1σ				
单辉橄榄岩 (18Tch02-2)																
1	23	298	239	0.8	0.0704	0.0007	0.5436	0.0103	0.0560	0.0010	439	4	441	8	453	38
2	330	988	193	0.2	0.3325	0.0034	5.2885	0.0699	0.1154	0.0013	1850	19	1867	25	1886	21
3	29	372	297	0.8	0.0706	0.0007	0.5469	0.0086	0.0562	0.0008	440	4	443	7	459	32
4	48	950	238	0.25	0.0520	0.0007	0.4208	0.0070	0.0586	0.0007	327	4	357	6	554	26
5	86	478	239	0.5	0.1735	0.0018	3.0001	0.0400	0.1254	0.0014	1031	10	1408	19	2035	20
6	12	107	46	0.43	0.1115	0.0014	0.9574	0.0216	0.0623	0.0013	682	8	682	15	683	44
7	30	391	289	0.74	0.0703	0.0007	0.5458	0.0083	0.0563	0.0008	438	4	442	7	464	31
8	53	461	245	0.53	0.1083	0.0013	1.0742	0.0193	0.0719	0.0010	663	8	741	13	984	28
9	59	778	503	0.65	0.0704	0.0007	0.5423	0.0074	0.0559	0.0007	439	5	440	6	446	26
10	45	588	510	0.87	0.0664	0.0010	0.5035	0.0104	0.0550	0.0009	414	6	414	9	413	36
11	54	1000	420	0.42	0.0514	0.0006	0.3843	0.0056	0.0542	0.0006	323	4	330	5	379	27
12	99	152	223	1.47	0.4485	0.0047	10.9572	0.1471	0.1772	0.0021	2388	25	2520	34	2627	19
13	157	463	84	0.18	0.3319	0.0038	5.2403	0.0745	0.1145	0.0013	1848	21	1859	26	1872	21
14	54	575	490	0.85	0.0768	0.0007	0.7286	0.0109	0.0688	0.0010	477	5	556	8	893	29
15	58	920	566	0.62	0.0560	0.0005	0.4204	0.0059	0.0545	0.0007	351	3	356	5	391	29
16	81	1221	551	0.45	0.0615	0.0006	0.4643	0.0063	0.0547	0.0007	385	4	387	5	400	27
17	28	376	225	0.6	0.0658	0.0007	0.4996	0.0084	0.0551	0.0008	411	4	411	7	416	34
18	18	217	183	0.84	0.0706	0.0007	0.5418	0.0102	0.0556	0.0010	440	4	440	8	438	39
19	97	1469	552	0.38	0.0614	0.0006	0.5433	0.0077	0.0641	0.0008	384	4	441	6	746	26
20	34	101	17	0.17	0.3329	0.0033	5.2186	0.0701	0.1137	0.0013	1852	18	1856	25	1859	21
21	37	112	12	0.1	0.3332	0.0034	5.2664	0.0751	0.1146	0.0014	1854	19	1863	27	1874	22
22	21	269	157	0.58	0.0708	0.0007	0.5467	0.0103	0.0560	0.0010	441	4	443	8	452	39
23	37	481	376	0.78	0.0664	0.0007	0.5071	0.0080	0.0554	0.0008	415	4	416	7	427	32
24	27	345	213	0.62	0.0705	0.0007	0.5453	0.0088	0.0561	0.0008	439	5	442	7	456	33
25	25	76	8	0.1	0.3319	0.0034	5.2708	0.0809	0.1152	0.0016	1847	19	1864	29	1883	25
26	111	1520	631	0.41	0.0706	0.0008	0.5412	0.0080	0.0556	0.0007	440	5	439	6	435	26
27	57	696	631	0.91	0.0704	0.0007	0.5431	0.0076	0.0559	0.0007	439	4	440	6	450	27
28	34	446	261	0.59	0.0706	0.0007	0.5457	0.0081	0.0561	0.0008	440	4	442	7	455	30
29	56	746	356	0.48	0.0708	0.0007	0.5472	0.0080	0.0561	0.0007	441	5	443	6	456	27
30	24	365	74	0.2	0.0702	0.0007	0.5382	0.0099	0.0556	0.0010	437	5	437	8	437	38
31	61	1530	227	0.15	0.0413	0.0004	0.3065	0.0043	0.0538	0.0006	261	3	271	4	362	27
32	68	935	348	0.37	0.0705	0.0007	0.5433	0.0077	0.0559	0.0007	439	5	441	6	447	27

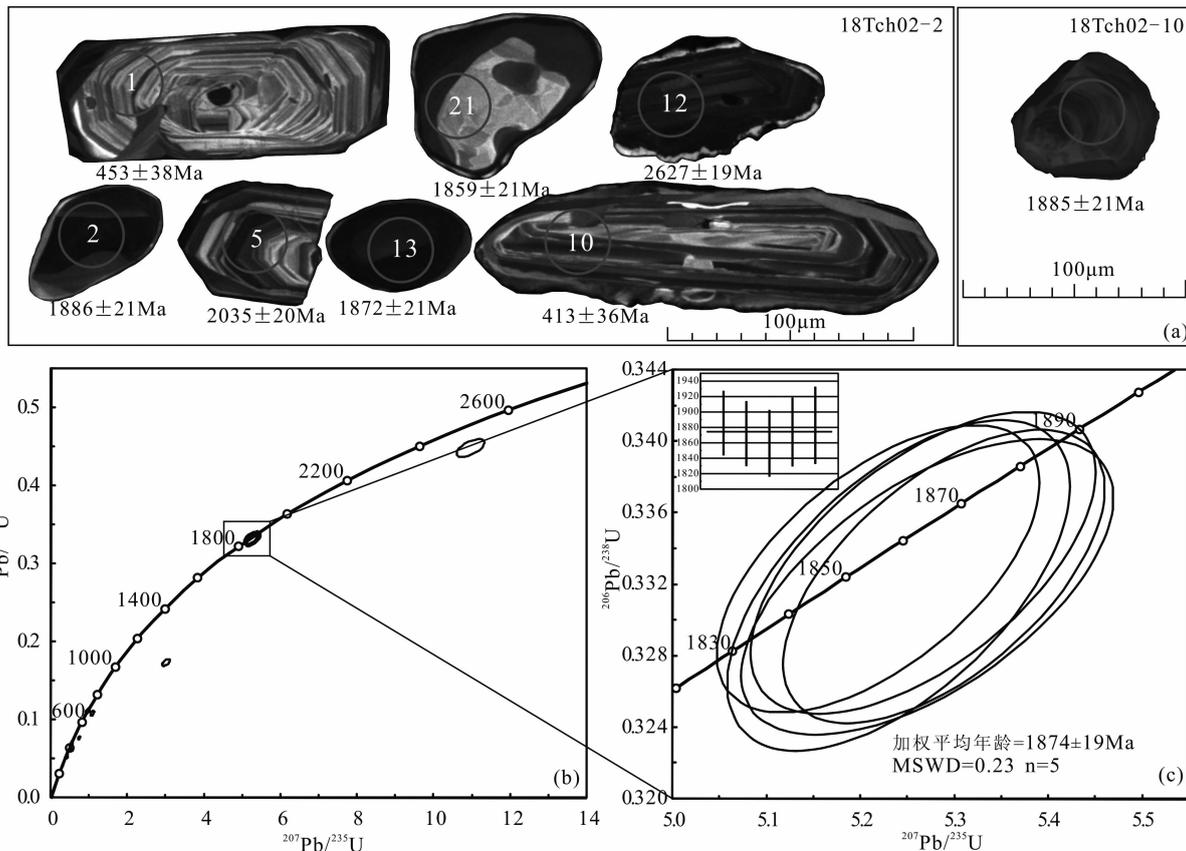


图 3 坦桑尼亚西南部 Nsamyia 杂岩体中单辉橄榄岩的锆石阴极发光图像(a)和 U-Pb 年龄谐和图(b,c)

Fig. 3 Climages(a) and U-Pb concordia age(b,c) of zircons from clinopyroxene peridotite in Nsamyia complex in southwestern Tanzania

4.2 岩石地球化学

4.2.1 主量元素

Nsamyia 岩体的全岩地球化学分析数据见表 3。

由于 Nsamyia 岩体的烧失量较大,为 2.51%~10.77%,主要与岩石的蚀变程度较强有关,需要对样品进行 100% 无水标准化计算。结果显示 SiO₂ 含量为 40.88%~48.82%,为基性-超基性系列, MgO、FeO_T、Al₂O₃、CaO 的含量变化较大, K₂O 与 Na₂O 总体含量较低, TiO₂ 含量也较低,都 <1%。其中,单辉橄榄岩的 MgO 含量较高(23.37%~35.57%), Al₂O₃ 含量较低(2.31%~5.14%), CaO 含量较低(2.01%~10.36%, 18Tch02-9 除外,为 14.59%), Mg[#] 为 79.9~83.5,明显低于蛇绿岩中变质橄榄岩的值(Mg[#] = 89~91)(Sun et al., 1989; Zhang Qi, 1992),而高于原始岩浆值(68~75, Wilson, 1989),反映了橄榄石和辉石的堆晶作用(Kohut et al., 2006; Yuan Lingling et al., 2017)。辉长岩的 MgO 含量较低(5.79%~13.34%), CaO 含量较高(14.61%~15.70%), Al₂O₃ 含量较高(13.81%~25.13%), Mg[#] 为 74.4

~78.8,主要与较多的单斜辉石、斜长石结晶有关,相对较高的 Mg[#] 表明岩石中有相当数量的早期堆晶相(橄榄石、辉石)存在。

在 FeO_T-MgO-Na₂O+K₂O 图上, Nsamyia 岩体的大部分样品落入弧堆晶岩区(图 4a)。在 Al₂O₃-MgO-CaO 图上,单辉橄榄岩和辉长岩分别投在超镁铁堆晶岩和镁铁堆晶岩范围内(图 4b),在 FeO_T-FeO_T/MgO 图解中,岩石多位于钙碱性范围内(图 4d)。在主量元素协变图上(图 5), SiO₂、Al₂O₃、CaO、Na₂O+K₂O 与 MgO 呈较好的负相关, FeO_T 和 MnO 为正相关, P₂O₅ 相对稳定,而 TiO₂ 随着岩浆演化先增高后降低,可能与含钛矿物(钛铁矿)在辉长岩演化过程中的先后结晶或围岩混染有关,整体显示岩石的化学成分变化受分离结晶作用控制,特别是受橄榄石和单斜辉石的影响。

4.2.2 微量元素

Nsamyia 基性-超基性岩体内单辉橄榄岩的 Cr 含量为 1480×10⁻⁶~2610×10⁻⁶, Ni 含量为 650×10⁻⁶~1780×10⁻⁶, Co 含量为 93×10⁻⁶~167×10⁻⁶, 整体含量较高,反映了岩体的堆晶性质(Cr>

表3 坦桑尼亚西南部乌本迪带 Nsamyia 岩体的主量元素(%)和微量元素($\times 10^{-6}$)分析结果Table 3 Major element (%) and trace element compositions ($\times 10^{-6}$) for Nsamyia rocks in the Ubendian Belt in southwestern Tanzania

样品号	18Tch02-1	18Tch02-2	18Tch02-3	18Tch02-4	18Tch02-5	18Tch02-7	18Tch02-9	18Tch02-6	18Tch02-8	18Tch02-10
样品名称	单辉橄榄岩							辉长岩		
SiO ₂	40.09	43.33	36.41	42.83	43.84	40.38	46.49	47.18	46.15	46.87
Al ₂ O ₃	4.65	2.76	4.58	2.72	3.06	2.11	2.75	13.39	24.39	17.24
Fe ₂ O ₃	8.48	7.6	11.75	6.63	5.7	9.05	5.45	1.37	1.36	2.37
FeO	4.36	3.07	2.47	3.42	5.42	3.23	3.83	4.98	2.14	4.22
CaO	6.6	9.46	1.79	9.32	9.76	6.77	13.89	15.22	14.18	13.73
MgO	26.65	26.47	31.68	26.59	25.81	29.38	22.25	12.93	5.62	10.34
K ₂ O	0.02	0.005	0.005	0.038	0.015	0.003	0.002	0.3	0.36	0.48
Na ₂ O	0.011	0.007	0.12	1.09	0.091	0.045	0.067	1.23	2.67	0.7
TiO ₂	0.15	0.32	0.085	0.25	0.29	0.2	0.3	0.21	0.098	0.24
P ₂ O ₅	0.011	0.014	0.01	0.013	0.013	0.012	0.01	0.013	0.012	0.022
MnO	0.32	0.2	0.16	0.15	0.19	0.15	0.18	0.12	0.068	0.11
灼失	8.16	6.43	10.77	6.57	5.22	8.3	4.35	2.51	2.7	3.21
Cu	5.31	19	386	8.13	8.64	5.68	9.74	17.4	129	89.3
Pb	1.84	0.91	0.5	0.38	0.35	0.37	0.37	0.66	1.58	1.23
Zn	81.3	76.1	90.3	58.8	74.5	74.4	54.1	55.5	28.4	43.5
Cr	1480	2390	2610	2500	2270	2540	2100	807	219	218
Ni	825	813	1780	976	747	943	650	268	114	142
Co	167	118	165	107	112	121	93	59	30.8	54.8
Rb	1.16	0.54	0.42	0.33	0.98	0.17	0.46	5.16	7.43	11.6
Cs	0.079	0.03	0.019	0.014	0.074	0.018	0.033	0.1	0.18	0.086
Sr	41.1	35.3	13.8	28.1	55.1	23.6	40	385	955	689
Ba	226	87.7	22.4	25.4	43.6	16.4	42	107	124	200
V	77.6	118	47.2	101	109	76.1	146	108	42.9	93.7
Sc	28.9	48.1	9.06	47.1	47.9	39.9	65.2	41.9	13.6	28.7
Nb	0.78	0.19	0.088	0.14	0.13	0.13	0.13	0.24	0.4	0.28
Ta	0.029	0.018	0.013	0.014	0.016	0.015	0.013	0.018	0.02	0.02
Zr	5.87	8.54	1.03	6.9	7.3	6.08	9.2	5.16	3.69	11.1
Hf	0.21	0.36	0.04	0.31	0.35	0.25	0.42	0.24	0.14	0.46
Be	0.18	0.076	0.032	0.054	0.086	0.039	0.1	0.07	0.11	0.2
Ga	7.91	4.66	3.21	2.88	3.72	2.42	3.8	8.15	11.6	12.9
U	0.27	0.047	0.18	0.032	0.029	0.016	0.038	0.016	0.02	0.052
Th	0.37	0.057	0.014	0.072	0.046	0.069	0.11	0.075	0.2	0.11
La	15	3.16	0.86	1.73	2.22	1.41	3.22	1.85	4.78	7.54
Ce	26.5	9.23	1.24	4.51	4.6	3.71	6.66	3.89	5	8.24
Pr	2.43	1.17	0.2	0.85	0.96	0.74	1.3	0.71	0.96	1.97
Nd	8.56	6.19	0.94	4.46	5.19	4.14	6.86	3.68	3.74	8.47
Sm	1.38	1.72	0.21	1.29	1.56	1.18	1.97	1.09	0.71	1.98
Eu	0.44	0.53	0.12	0.38	0.47	0.35	0.58	0.44	0.42	0.72
Gd	1.46	1.53	0.2	1.04	1.26	0.97	1.71	1.02	0.68	1.67
Tb	0.21	0.26	0.031	0.19	0.23	0.16	0.29	0.18	0.1	0.28
Dy	1.04	1.45	0.18	1.03	1.3	0.88	1.64	1.13	0.54	1.53
Ho	0.2	0.27	0.036	0.2	0.24	0.16	0.3	0.22	0.093	0.28
Er	0.58	0.74	0.1	0.52	0.63	0.4	0.78	0.62	0.26	0.76
Tm	0.075	0.1	0.018	0.072	0.094	0.054	0.12	0.088	0.036	0.11
Yb	0.47	0.59	0.11	0.42	0.53	0.31	0.66	0.55	0.2	0.68
Lu	0.07	0.086	0.02	0.065	0.081	0.045	0.099	0.087	0.03	0.097
Y	5.39	6.93	1.3	4.79	5.98	3.72	7.34	5.57	2.37	7.19
Mg [#]	79.9	82.7	81.3	83.5	81.4	82.2	82	78.8	74.9	74.4
∑REE	58.42	27.03	4.27	16.76	19.37	14.51	26.19	15.56	17.55	34.33
(La/Yb) _N	21.52	3.61	5.27	2.78	2.82	3.07	3.29	2.27	16.11	7.48
δEu	0.96	1.15	0.7	0.89	0.76	0.87	0.78	0.82	0.53	0.5

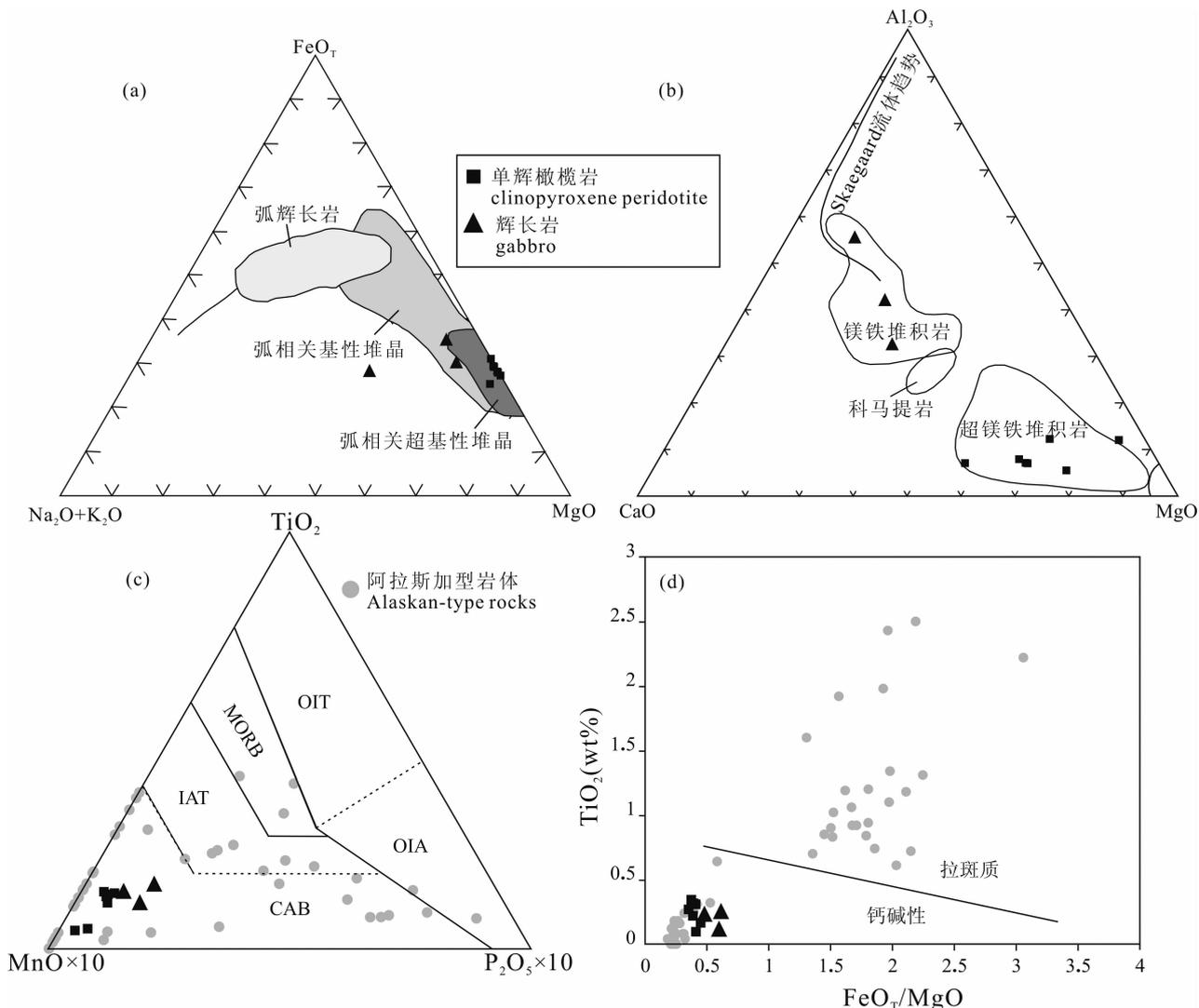


图 4 Nsamyia 杂岩体 FeO_T - MgO - Na_2O+K_2O 图(a, 据 Beard, 1986), Al_2O_3 - MgO - CaO 图(b, 据 Coleman, 1977), TiO_2 - MnO - P_2O_5 图(c, 据 Mullen, 1983) 和 TiO_2 - FeO_T/MgO 图(d, 据 Miyashiro, 1975)

Fig. 4 The diagrams of FeO_T - MgO - Na_2O+K_2O (a, after Beard, 1986), Al_2O_3 - MgO - CaO (b, after Coleman, 1977), TiO_2 - MnO - P_2O_5 (c, after Mullen, 1983) and TiO_2 - FeO_T/MgO (d, after Miyashiro, 1975)

MORB—大洋中脊玄武岩; IAT—岛弧拉斑质玄武岩; CAB—岛弧钙碱性玄武岩; OIT—海山拉斑质玄武岩; OIA—海山碱性玄武岩
MORB—mid-ocean ridge basalt; IAT— island arc tholeiite; CAB— island arc calc-alkaline;
OIT— seamount tholeiite; OIA— seamount alkalic

1000×10^{-6} , $Ni > 300 \times 10^{-6}$; Roberts et al., 2000; Polat et al., 2011, 2012; Dong Jinlong et al., 2018), Cr, Ni 和 Co 与 MgO 呈正相关性(图 5),反映了橄榄石和辉石的分离结晶。单辉橄榄岩的 REE 总量较低($\Sigma REE = 4.27 \times 10^{-6} \sim 27.03 \times 10^{-6}$),仅 1 个样品含量较高,为 58.42×10^{-6} 。在球粒陨石标准化的 REE 配分图上(图 6b),具有微弱分异的右倾 REE 分布模式, $LREE/HREE = 3.44 \sim 13.23$, $(La/Yb)_N = 2.78 \sim 21.52$, $(La/Sm)_N = 0.75 \sim 6.84$, $(Gd/Yb)_N = 1.47 \sim 2.52$,表明稀土的分馏弱到中等。除 1 个样品具有铕异常(δEu

$= 1.77$)外,其他样品的铕异常不明显,其 δEu 值为 $0.94 \sim 0.99$ 。在原始地幔标准化的微量元素图解上(图 6a),略富集 LILE(Ba, Pb, U),亏损 HFSE(Nb, Ta, Zr, Hf, Ti 和 Y),表明与俯冲作用或大陆地壳物质具有一定的亲缘性。

辉长岩的 Cr, Ni 和 Co 元素含量相对前者要低,分别为 $218 \times 10^{-6} \sim 807 \times 10^{-6}$, $114 \times 10^{-6} \sim 268 \times 10^{-6}$ 和 $30.8 \times 10^{-6} \sim 59 \times 10^{-6}$,反映了岩浆演化过程中橄榄石和辉石的结晶分异作用。在球粒陨石标准化的 REE 配分图上(图 6b),具有与单辉橄榄岩相似的分配模式, $LREE/HREE = 2.99 \sim$

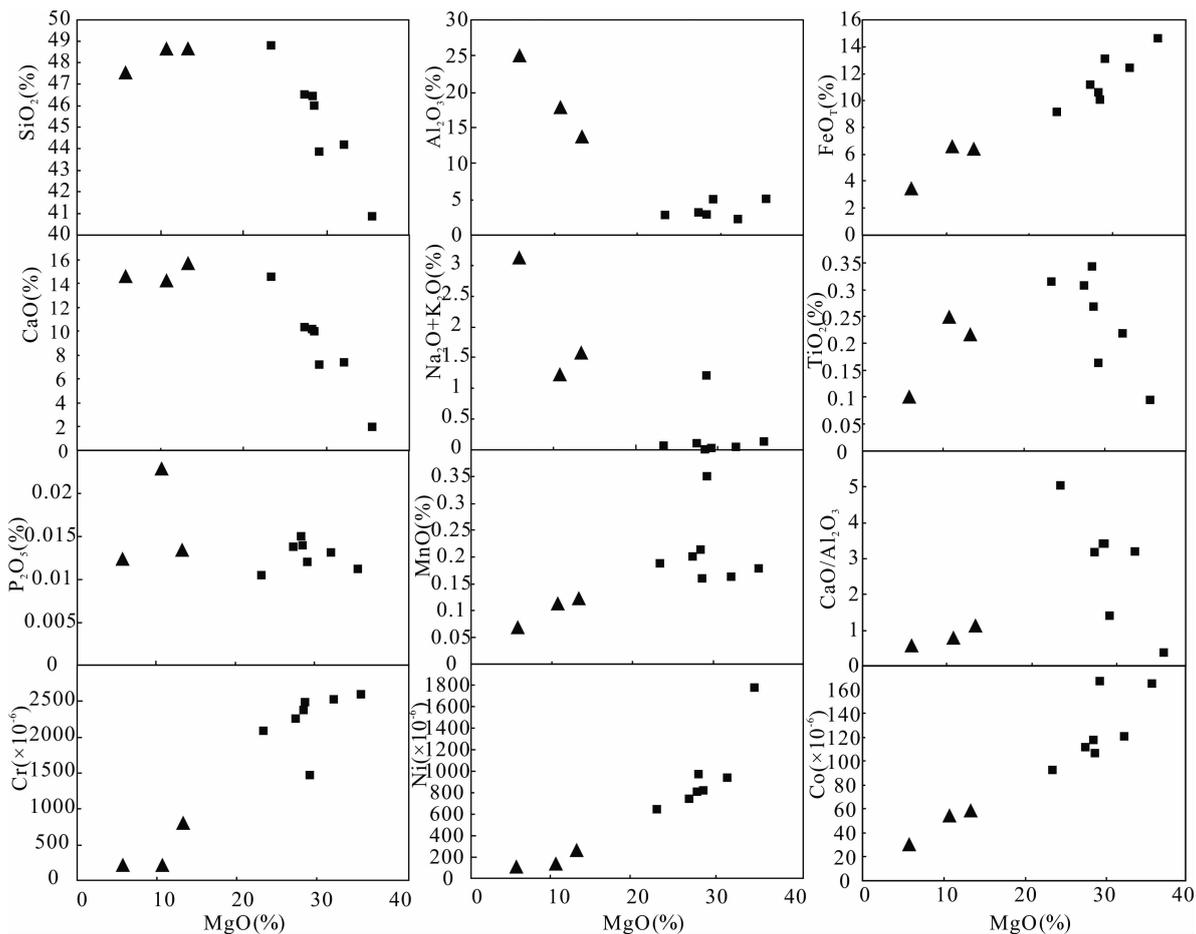


图5 坦桑尼亚西南部 Nsamya 杂岩体 MgO-其他元素协变图

Fig. 5 Plots of MgO vs. other elements of Nsamya complex in southwestern Tanzania showing element variations with fractional crystallization

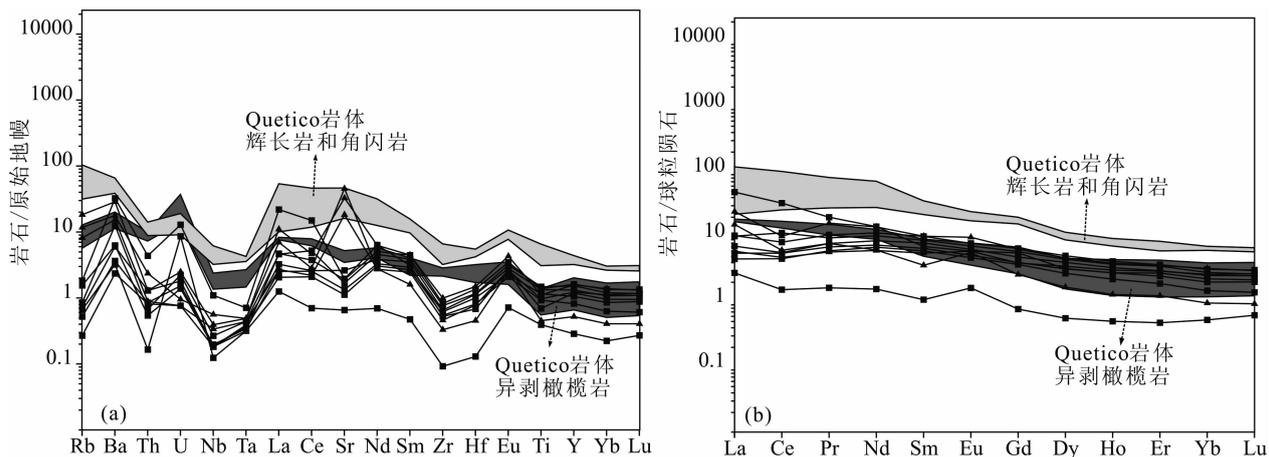


图6 坦桑尼亚西南部 Nsamya 杂岩体原始地幔标准化微量元素蛛网图(a)和球粒陨石标准化稀土元素配分图(b)

Fig. 6 Primitive mantle-normalized trace-element patterns (a) and chondrite-normalized REE patterns (b) of Nsamya complex in southwestern Tanzania

阿拉斯加型 Quetico 岩体数据引自 Pettigrew et al. (2006); 标准化数据引自 Sun et al. (1989)

The data of Alaskan-type Quetico rocks are after Pettigrew et al. (2006), and primitive mantle and chondrite after Sun et al. (1989)

8.05, $(La/Yb)_N = 2.27 \sim 16.11$, $(La/Sm)_N = 1.07 \sim 4.23$, $(Gd/Yb)_N = 1.50 \sim 2.74$ 。辉长岩具有钕正异常 ($\delta Eu = 1.26 \sim 1.82$), 与斜长石的堆晶作用有关。在原始地幔标准化的微量元素图解上 (图 6a), 与单辉橄榄岩的特征总体相似, 指示其为同源岩浆演化的产物。

Nsamyia 杂岩体的各类岩石的 REE 和微量元素特征可与典型的阿拉斯加型杂岩体—Quetico 杂岩体类比 (Pettigrew et al., 2006) (图 6), 其明显的 Nb、Ta、Y、Zr、Hf 和 Ti 负异常显示出与俯冲带相关岩浆的特征, 因此可以推测该杂岩体为弧岩浆分离结晶的产物。

5 讨论

5.1 岩浆源区和岩浆演化

基性-超基性岩体的岩浆源区是多样的, 包括活动大陆边缘环境、造山后伸展环境 (Ao S J et al.,

2010; Deng Yufeng et al., 2011) 及裂谷或地幔柱活动环境 (Trun et al., 1996; Zhang Chuanlin et al., 2010)。Nsamyia 基性-超基性杂岩体具有高 Mg、Cr、Ni 和 Co 等特征, 表明该杂岩体具有幔源特征 (Wilson, 1989; Cox et al., 1980; Qin Kezhang et al., 2018)。富集 LREE 和 Ba、Pb、U 等大离子亲石元素, 不同程度的亏损 HREE 和 Nb、Ta、Zr、Hf 和 Ti 等高场强元素特征, 表明该杂岩体具有弧岩浆特征 (Kelemen, 1990; Hawkesworth et al., 1993; Su Benxun et al., 2012)。在 La/Ba-La/Nb 图解中 (图 7a), 岩石均投点于俯冲交代岩石圈地幔区 (Woodhead et al., 2001)。不相容元素因分配系数相似, 其比值受分离结晶作用的影响较小, 在地幔部分熔融过程中变化小, 对源区有一定的指示意义 (Woodhead et al., 2001; Hu Chaobin et al., 2018; Jiao Jiangang et al., 2017)。研究认为, Tb/Yb 比值高暗示部分熔融程度相对较低, 源区的主

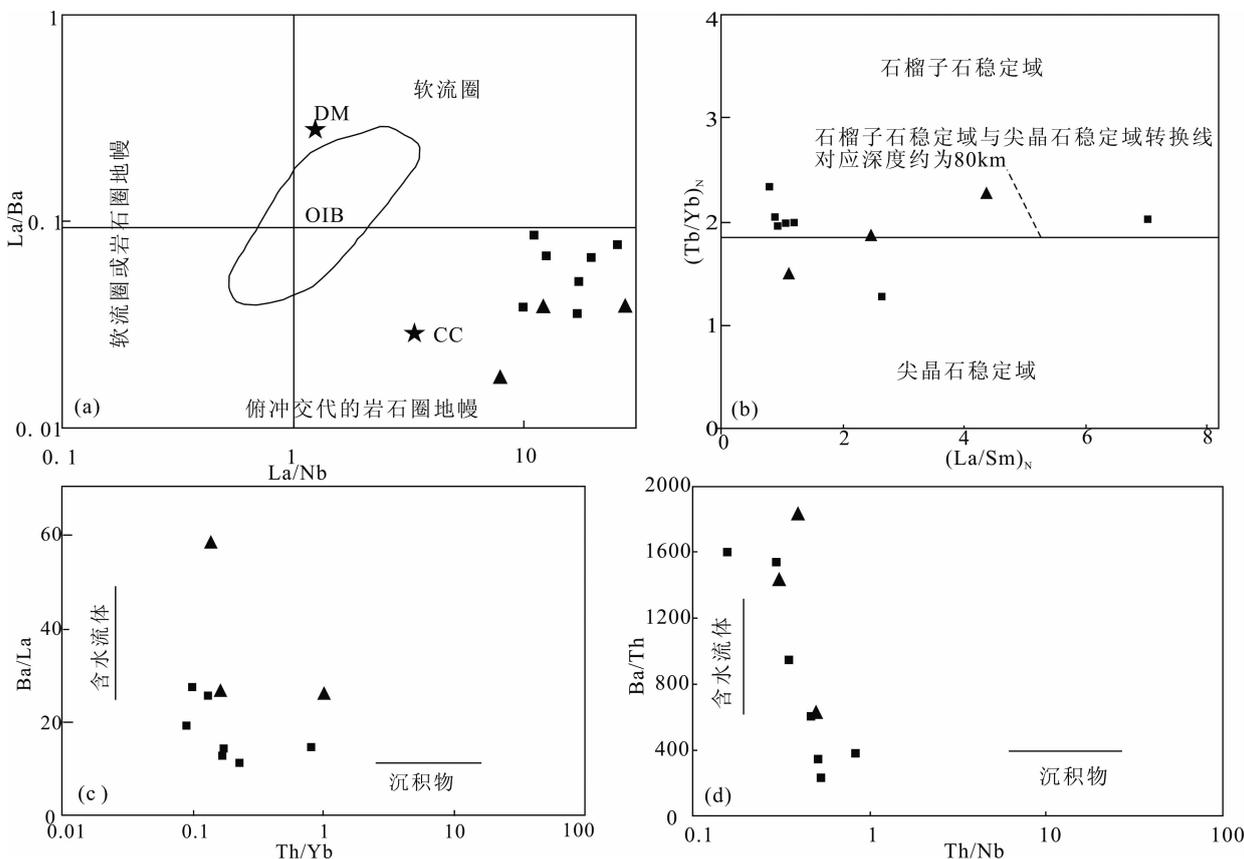


图 7 坦桑尼亚西南部 Nsamyia 杂岩体 La/Ba-La/Nb(a, 据 Fitton et al., 1991)、 $(Tb/Yb)_N$ - $(La/Sm)_N$ (b, 据 Wang K et al., 2002)、

Ba/La-Th/Yb 和 Ba/Th-Th/Nb(c, d, 据 Woodhead et al., 2001) 图解

Fig. 7 La/Ba-La/Nb (a, after Fitton et al., 1991)、 $(Tb/Yb)_N$ - $(La/Sm)_N$ (b, after Wang K et al., 2002)、Ba/La-Th/Yb and Ba/Th-Th/Nb (c, d, after Woodhead et al., 2001) diagrams of Nsamyia complex in southwestern Tanzania

要残留相为石榴子石; Tb/Yb 比值低暗示部分熔融程度相对较高, 源区的主要残留相为尖晶石 (Wang K et al., 2002; Zhang Xiaohui et al., 2008; Jiao Jiagang et al., 2017)。在 $(\text{Tb}/\text{Yb})_{\text{N}}-(\text{La}/\text{Sm})_{\text{N}}$ 图解中, 岩石大部分落入石榴子石稳定区域 (图 7b), 其 Tb/Yb 比值位于 0.28~0.52 之间, 平均值为 0.43, 高于俯冲成因的东天山黄山西地区和甘肃龙首山地区的镁铁-超镁铁岩体 (Deng Yufeng et al., 2011; Jiao Jiagang et al., 2017), 且 Cr、Ni 含量低于熔融程度较高的龙首山地区杂岩体, 暗示岩浆源区部分熔融程度相对较低。受俯冲板块熔体相互作用最终形成的镁铁质岩浆通常具有相对富碱、高 P_2O_5 和 TiO_2 含量的特征 (Sajona et al., 2000), 而 Nsamyia 杂岩体大部分具钙碱性特征, 且 TiO_2 含量低, 说明俯冲板块熔体的交代作用有限。利用微量元素比值 (Ba/Th, Th/Nb, Ba/La 和 Th/Yb) 可识别俯冲带沉积物和含水流体对岩石圈地幔交代作用的影响。本次研究岩石均具有相对稳定的 Th/Nb 和 Th/Yb 比值 (0.16~0.85, 0.09~1), 变化范围较大的 Ba/Th 和 Ba/La 比值 (238~1818, 11.63~57.84), 指示了含水流体对岩石圈地幔的交代作用 (图 7c, d; Woodhead et al., 2001; Hanyu et al., 2006; Hu Chaobin et al., 2018)。

Nsamyia 杂岩体平面形态呈椭圆状, 与 Lwerianga-Sowanyeri、Mwansanga 等变质辉长岩体和其他的小型露头沿 Usangu 剪切带呈线性分布, 岩性由中心向边缘依次为橄榄岩-橄榄辉石岩-辉长岩, 这些特征与世界上典型的阿拉斯加型杂岩体相似 (Guillou-Frottier et al., 2014; Taylor, 1967; Irvine, 1974; Himmelberg et al., 1995; Burg et al., 2009; Tessalina et al., 2016; Cai Keda et al., 2012; Su Benxun et al., 2012, 2014; Pettigrew et al., 2006; Helmy et al., 2003; Helmy et al., 2014)。地球化学方面, 其 SiO_2 含量低 (平均值为 46.17%), MgO 、 FeO_T 含量高, TiO_2 含量低, $\text{Mg}^\#$ 高, 元素特征及稀土、微量元素的标准化配分模式具有阿拉斯加型杂岩体的性质 (图 6)。在主量元素判别图解 $\text{MnO}-\text{TiO}_2-\text{P}_2\text{O}_5$ 图解上 (Mullen, 1983), Nsamyia 杂岩体与阿拉斯加型杂岩体位于相似的区域 (图 4c)。早期研究表明, 阿拉斯加型侵入杂岩体的母岩浆多为苦橄质、含水岩浆 (Loucks, 1990; Loney et al., 1992; Helmy et al., 2003; Pettigrew et al., 2006), 因此 Nsamyia 杂岩体可能为含水的苦橄质岩浆分离结晶的早期堆晶

产物。

苦橄质岩浆的分离结晶过程可能伴随有地壳物质的混染 (AFC 过程, DePaolo, 1981; Hu Chaobin et al., 2018), AFC 过程的主要标志是由于地壳组分的加入和随着岩浆演化程度的升高 (SiO_2 含量升高和 $\text{Mg}^\#$ 值降低), 会导致不相容元素 (如高场强元素) 含量的同步降低 (He Qi et al., 2009)。而总分配系数相同或相近的元素不受分离结晶和部分熔融程度的影响, 可以用这些元素的比值的协变关系来分析岩浆的同化混染, 并判断混染程度, 如 Ce/Pb、Th/Zr、La/Nb、Nb/Ta、Ta/Yb、Th/Yb 和 Zr/Nb 等 (Baker et al., 1997; MacDonald et al., 2001)。该岩体 Nb/La 和 Th/Nb 元素比值与 $\text{Mg}^\#$ 之间协同变化关系不明显 (图 8), 指示同化混染作用较弱。除 2 个样品外 (La/Sm 为 10.87 和 6.73), 其他样品的 La/Sm = 1.19~4.10, 均小于 4.5 (地壳物质混染: La/Sm > 4.5; Sun et al., 1989; Hu Chaobin et al., 2018; Chai Fengmei et al., 2007)。结合样品中含有捕获的太古宙锆石, 认为 Nsamyia 岩体在分离结晶过程中受同化混染作用的影响是不均匀的或者是少量的。岩体中所有样品的 Th 含量极低 ($0.04 \times 10^{-6} \sim 0.2 \times 10^{-6}$), 表明岩浆中加入的是岩石圈或下地壳物质 (Th 含量低, 平均值为 1.2×10^{-6}), 而不是上地壳物质 (Th 含量高, 平均值为 10.7×10^{-6}) (Taylor et al., 1985; Chai Fengmei et al., 2007)。Neal et al. (2002) 提出可以用 $(\text{La}/\text{Nb})_{\text{PM}}$ 和 $(\text{Th}/\text{Ta})_{\text{PM}}$ 值来区分上地壳和下地壳物质的混染作用, 在图 9 中大部分样品点靠近下地壳范围, 结合捕获的太古宙锆石年龄, 表明混染物主要为下地壳太古宙基底组分 (Xu Kangkang et al., 2019, 2020)。由此可见, Nsamyia 基性-超基性岩体为俯冲板块流体交代岩石圈地幔, 导致部分熔融形成苦橄质岩浆, 在上升过程中受太古宙地壳混染作用而结晶的早期堆晶产物。

5.2 地质年龄及构造意义

研究区位于坦桑尼亚克拉通的西南地区, 新太古宙时期发育有大规模的基性-花岗质岩浆的侵入作用, 构成了乌本迪带的太古宙基底 (Manya, 2011; Lawley et al., 2013; Kazimoto et al., 2014)。至古元古代时期, 乌本迪带开始了早期的洋壳俯冲作用 (Boniface et al., 2012; Zuo Libo et al., 2020)。

已有的同位素资料表明, 在 Katuma 地质单元中基性岩浆的锆石 U-Pb 年龄为 $2021 \pm 11\text{Ma}$

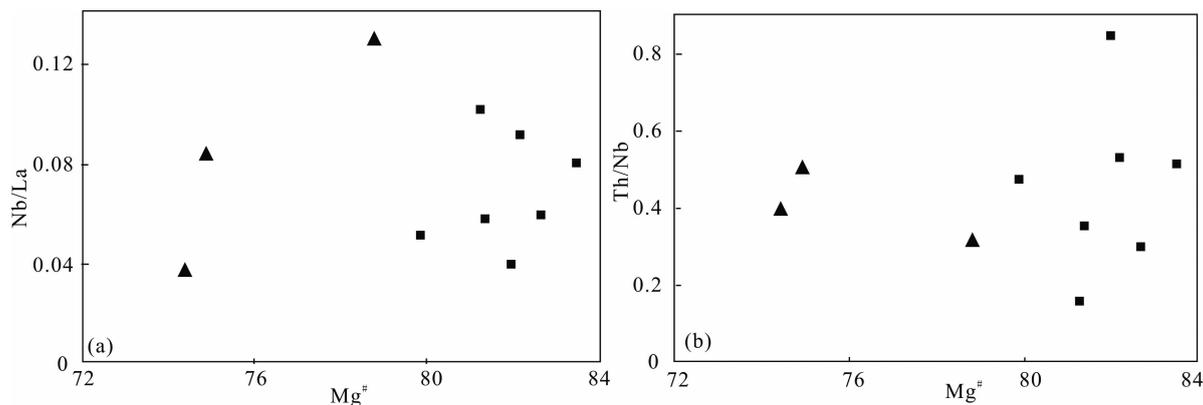


图 8 坦桑尼亚西南部 Nsamyia 杂岩体 Ba/La-Mg[#] (a) 和 Th/Nb-Mg[#] (b) 图解

Fig. 8 Ba/La-Mg[#] (a) and Th/Nb-Mg[#] (b) diagrams of Nsamyia complex in southwestern Tanzania

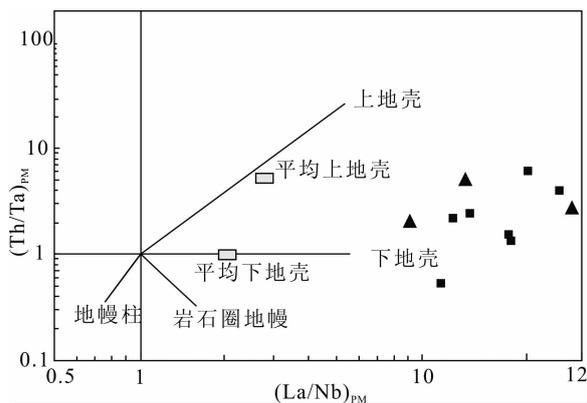


图 9 坦桑尼亚西南部 Nsamyia 杂岩体
(Th/Ta)_{PM}-(La/Nb)_{PM} 图解

Fig. 9 (Th/Ta)_{PM}-(La/Nb)_{PM} diagram of Nsamyia complex in southwestern Tanzania

(Kazimoto et al., 2015);Lupa 地质单元内 Saza 花岗闪长岩和 Ngualla 玄武质安山岩的锆石 U-Pb 年龄分别为 1930 ± 3Ma 和 1943 ± 32Ma (Lawley et al., 2013; Tulibonywa et al., 2015);Katuma 地质单元中混合岩化正片麻岩和其内浅色体的锆石 U-Pb 年龄为 2030~2050Ma, Ikulu 群泥质混合岩中浅色体的变质锆石 U-Pb 年龄为 1940~1960Ma (Kazimoto et al., 2014)。这些年龄可能代表了乌本迪造山运动早阶段的岩浆作用和变质作用。

Boniface et al., (2012) 通过研究发现在 Ubende 地质单元内存在 MORB 性质的榴辉岩, 其变质锆石年龄为 1886 ± 16Ma 和 1866 ± 14Ma, 推测乌本迪带存在古元古代的俯冲事件。其他地质单元内同期的岩浆变质作用包括: Ufipa 地质单元内花岗岩的锆石 U-Pb 年龄为 1847 ± 37Ma 和 1864 ± 32Ma (Lenoir et al., 1994); Lupa 地质单元内花岗岩和斑状英安岩的锆石 U-Pb 年龄分别为 1878 ±

15Ma 和 1871 ± 5Ma (Tulibonywa et al., 2015, 2017); Katuma 地质单元内变质泥岩中独居石的变质边缘 U-Th-Pb 年龄为 1837 ± 6Ma 和 1848 ± 16Ma (Kazimoto et al., 2015); Ubende 地质单元内变质泥岩中独居石和锆石的 U-Pb 年龄分别为 1831 ± 11Ma 和 1817 ± 26Ma (Boniface et al., 2012)。这些年龄可能代表了乌本迪造山运动晚阶段的岩浆作用和变质作用。

本次获得的 Nsamyia 杂岩体的结晶年龄介于 1874~1944Ma 之间, 可能为 1885 ± 21Ma, 结合前人有关俯冲岩体的年龄研究, 可以推测阿拉斯加型的 Nsamyia 杂岩体代表了洋壳俯冲晚阶段的产物。利用抗蚀变能力强, 且不受分离结晶作用影响的元素相关性图解来判断构造环境, Nsamyia 杂岩体均落入大洋岛弧环境、火山弧区域内(图 10)。研究发现, 阿拉斯加型侵入体通常分布于前寒武纪晚期和显生宙的造山带内, 如南美和北美的科迪勒拉山脉 (Taylor, 1967; Irvine, 1974; Tistl, 1994), 乌拉尔山脉 (Fershtater et al., 1997) 和埃塞俄比亚西部的东非造山带 (Grenne et al., 2003)。基于对阿拉斯加地区 Duke 岛杂岩体详细的构造学研究, Saleeby (1992) 认为阿拉斯加型侵入体可能在弧内盆地闭合期间侵入, 与 Alexander 地体增生到北美陆块的最晚阶段相对应 (Foley et al., 1997)。埃塞俄比亚西部的阿拉斯加型岩体具有相似的构造背景, 为陆-陆碰撞阶段之前莫桑比克洋壳俯冲作用阶段的产物 (Worku et al., 1996; Grenne et al., 2003)。据此, 推测 Nsamyia 杂岩体的形成环境可能为岛弧内盆地环境, 为俯冲晚期岩浆作用产物。同时, 根据乌本迪带内榴辉岩和阿拉斯加型 Nsamyia 杂岩体的空间分布特征, 可知古元古代乌本迪造山阶段洋壳的俯冲

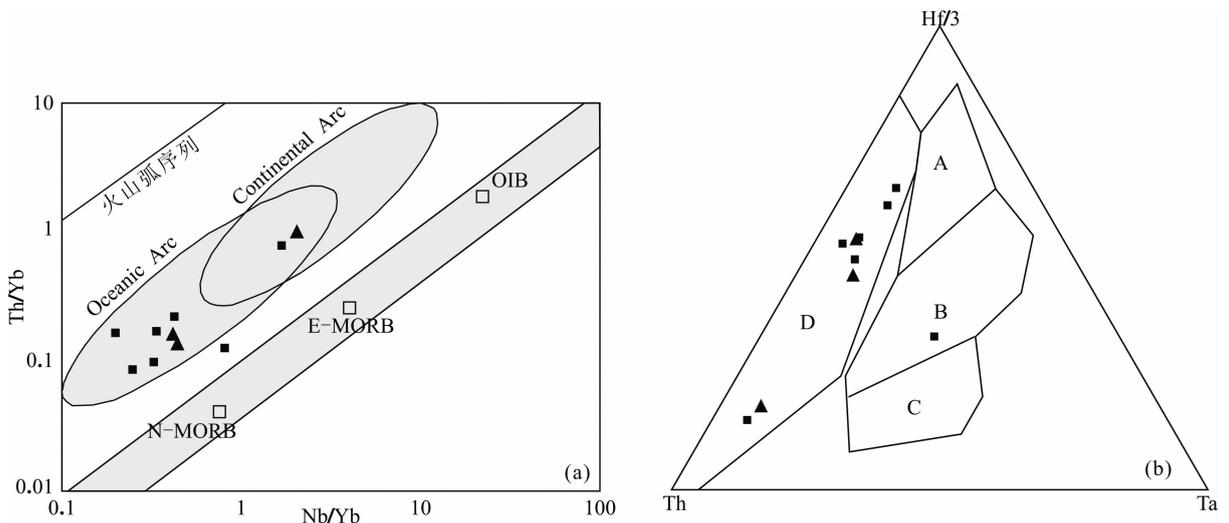


图 10 坦桑尼亚西南部 Nsamya 杂岩体 Th/Yb vs. Nb/Yb(a, 据 Pearce, 2014)和 Hf-Th-Ta(b, 据 Wood, 1980)判别图解
Fig. 10 Tectonic discrimination diagrams of Th/Yb vs. Nb/Yb(a, after Pearce, 2014)和 Hf-Th-Ta(b, after Wood, 1980)
of Nsamya complex in southwestern Tanzania

A—正常洋中脊玄武岩; B—板内拉板玄武岩+富集型洋中脊玄武岩; C—板内碱性玄武岩; D—火山弧玄武岩
A—N-MORB; B—WPB+E-MORB; C—WPB; D—VAB

方向为 NE 向,该结论为乌本迪带古元古代的板块运动提供了新的证据。

6 结论

(1) 出露于乌本迪带 Lupa 地质单元内的 Nsamya 镁铁-超镁铁质杂岩体具环形构造特征,为钙碱性系列,岩性主要包括单辉橄榄岩、橄榄辉石岩和辉长岩等,通过单辉橄榄岩中锆石 U-Pb 定年得到岩体的形成年龄介于 1784~1944Ma 之间,可能为 1885 ± 21 Ma,为古元古代晚期。

(2) 岩石具有高 $Mg^{\#}$ 等特征,为早期堆晶岩石,且富集 LREE 和 Ba、Pb、U 等大离子亲石元素,不同程度的亏损 HREE 和 Nb、Ta、Zr、Hf 和 Ti 等高场强元素,为具有弧岩浆特征的阿拉斯加型镁铁-超镁铁质杂岩体。

(3) 原生岩浆为苦橄质岩浆组分,起源于受板块流体交代的岩石圈地幔,在岩浆演化过程中受到下地壳太古宙基底岩石的混染作用。

(4) Nsamya 镁铁质-超镁铁质杂岩体形成于洋壳向 NE 方向俯冲的晚期阶段,形成于岛弧内盆地环境。

References

Ao S J, Xiao W J, Han C M, Mao Q G, Zhang J E. 2010. Geochronology and geochemistry of Early Permian mafic-ultramafic complexes in the Beishan area, Xinjiang, NW China: Implications for late Paleozoic tectonic evolution of the southern

Altoids. *Gondwana Research*, 18(2): 466~478.
Baker J A, Menzies M, Thirlwall M F, Macpherson C G. 1997. Petrogenesis of Quaternary Intraplate Volcanism, Sana'a, Yemen: Implications for Plume-Lithosphere Interaction and Polybaric Melt Hybridization. *Journal of Petrology*, 38(10): 1359~1390.
Batanova V C, Pertsev A N, Kamenetsky V S, Ariskin A A, Mochalov A G, Sobolev A V. 2005. Crustal evolution of island-arc ultramafic magma: Galmoenan pyroxenite-dunite plutonic complex, Koryak, Highland (Far East Russia). *Journal of Petrology*, 46(7): 1345~1366.
Beard J S. 1986. Characteristic mineralogy of arc-related cumulate gabbros: implications for the tectonic setting of gabbroic plutons and for andesite genesis. *Geology* 14(10): 848~851.
Belousova E, Griffin W L, O'Reilly S Y, Fisher N L. 2002. Igneous zircon: trace element composition as an indicator of source rock type. *Contributions to mineralogy and petrology*, 143(5): 602~622.
Boniface N, Schenk V, Appel P. 2012. Paleoproterozoic eclogites of MORB-type chemistry and three Proterozoic orogenic cycles in the Ubendian Belt (Tanzania): Evidence from monazite and zircon geochronology, and geochemistry. *Precambrian Research*, 192: 16~33.
Boniface N, Appel P. 2017. Stenian-Tonian and Ediacaran metamorphic imprints in the southern Paleoproterozoic Ubendian Belt, Tanzania: Constraints from in situ monazite ages. *Journal of African Earth Sciences*, 133: 25~35.
Burg J P, Bodinier J L, Gerya T, Bedini R M, Boudier F, Dautria J M, Prikhodko V, Efimov A, Pupier E, Balanec J L. 2009. Translithospheric mantle diapirism: geological evidence and numerical modelling of the Kondyor zoned ultra-mafic complex (Russian Far-East). *J. Petrol.* 50: 289~321.
Cai Keda, Sun Min, Yuan C, Zhao Guochun, Xiao Wenjiao, Long Xiaoping. 2012. Keketuohai maficultramafic complex in Chinese Altai, NW China: petrogenesis and geodynamics significance. *Chemical Geology*. 294~295: 26~41.
Chai Fengmei, Zhang Zhaochong, Dong Lianhui, Zhang Zuoheng, Wu Hua, Li Jun. 2007. Geochemistry and petrogenesis of the Baishiquan Cu-Ni sulfide-bearing mafic-ultramafic intrusion in the Central Tianshan, Xinjiang, NW China. *Acta Petrologica Sinica*, 23(10): 48~60 (in chinese with English abstract).

- Coleman R G. 1977. Ophiolites- Ancient Oceanic Lithosphere? Berlin: Springer Verlag.
- Cox K G. A model for flood basalt volcanism. *Journal of Petrology*, 1980, 21: 625~650.
- Daly M C, Klerkx J, Nanyaro J T. 1985. Early Proterozoic terranes and strike-slip accretion in the Ubendian Belt of southwest Tanzania. *Terra Cognita*, 5: 1~257.
- Daly M C. 1988. Crustal shear zones in Central Africa: a kinematic approach to Proterozoic Tectonics. *Episodes*, 11(1): 5~11.
- Debari S M, Coleman R G. 1989. Examination of the deep levels of an island arc; evidence from the Tonsina ultramafic-mafic assemblage, Tonsina, Alaska. *J. Geophys. Res.* 94: 4373~4391.
- Deng Yufeng, Song Xieyan, Chen Liemeng, Cheng Songlin, Zhang Xinli, Li Jun. 2011. Features of the mantle source of the Huangshanxi Ni-Cu sulfide-bearing mafic-ultramafic intrusion, eastern Tianshan. in *Acta Petrologica Sinica*, 27(12): 3640~3652 (in chinese with English abstract).
- DePaolo D J. 1981. Trace element and isotopic effects of combined wallrock assimilation and fractional crystallization. *Earth and Planetary Science Letters*, 53(2): 189~202.
- Dong Jinlong, Song Shuguang, Wang Mingming, Mark B A, Su Li, Wang Chao, Yang Liming, Xu Bei. 2018. Alaskan-type Kedanshan intrusion (central Inner Mongolia, China): Superimposed subduction between the Mongol-Okhotsk and Paleo-Pacific oceans in the Jurassic[J]. *Journal of Asian Earth Sciences*, 167: 68~81.
- Eyuboglu Y, Dilek Y, Bozkurt E, Bektas O, Rojay B, Sen C. 2010. Structure and geochemistry of an Alaskan-type ultramafic-mafic complex in the Eastern Pontides, NE Turkey. *Gondwana Res.* 18: 230~252.
- Eyuboglu Y, Dilek Y, Bozkurt E, Bektas O, Rojay B, Sen C. 2010. Structure and geochemistry of an Alaskan-type ultramafic-mafic complex in the Eastern Pontides, NE Turkey. *Gondwana Res.* 18(1): 230~252.
- Feng Yanqing, Qian Zhuangzhi, Duan Jun, Sun Tao, Xu Gang, Jiang Chao, Ren Meng, Chen Hongjun. 2017. Genesis and Ore-forming Potential of Mafic-Ultramafic Intrusions in the Western Part of East Tianshan Cu-Ni Metallogenic Belt, Xinjiang. *Acta Geologica Sinica*, 91(4): 792~811 (in chinese with English abstract).
- Fershtater G B, Montero P, Borodina N S, Pushkarev E V, Smirnov V N, Bea F. 1997. Uralian magmatism: an overview[J]. *Tectonophysics*, 276(1): 87~102.
- Fitton J G, James D, Leeman W P. 1991. Basic magmatism associated with late Cenozoic extension in the Western United States; Compositional variations in space and time. *Journal of Geophysical Research*, 96(B8): 13693~13711.
- Foley J P, Light T D, Nelson S W, Harris R A. 1997. Mineral occurrences associated with mafic-ultramafic and related alkaline complexes in Alaska. *Economic Geology*, 9: 396~449.
- Grenne T, Pedersen R B, Bjerkgard T, Braathen A, Selassie M G, Worku T. 2003. Neoproterozoic evolution of western Ethiopia: igneous geochemistry, isotope systematics and U-Pb ages. *Geological Magazine*, 140(4): 373~395.
- Guillou-Frottier L, Burov E, Ahge T, Gloaguen E. 2014. Rheological conditions for emplacement of Ural-Alaskan-type ultramafic complexes. *Tectonophysics* 631: 130~145.
- Hanyu T, Tatsumi Y, Nakai S, Chang Q, Miyazaki T, Sato K, Tani K, Shibata T, Yoshida T. 2006. Contribution of slab melting and slab dehydration to magmatism in the NE Japan arc for the last 25 Myr; Constraints from geochemistry, geochemistry geophysics geosystems, 7(8): 1~29.
- Hawkesworth C J, Gallagher K, Hergt J M, McDermott F. 1993. Mantle and slab contributions in arc magmas. *Annual Review of Earth and Planetary Sciences*, 21: 175~204.
- He Qi, Xiao Long, Wei Qirong, Ni Pingze. 2009. Petrological and geochemical characteristics of the Jiyidu ophiolitic mélange, West Yunnan; Constraints for its tectonic implications. *Acta Petrologica Sinica*, 25(12): 3229~3240.
- Helmy H M, AbdYasser M, El-Rahman Y M, Yoshikawa M, Shibata T, Arai S, Tamura A, Kagami H. 2014. Petrology and Sm-Nd dating of the Genina Gharbia Alaskan-type complex (Egypt): insights into deep levels of Neoproterozoic island arcs. *Lithos* (198~199): 263~280.
- Helmy H M, ElMahallawi M M. 2003. Gabbro Akarem mafic-ultramafic complex, Eastern Desert, Egypt: a late Precambrian analogue of Alaskan-type Complexes. *Mineral. Petrol.* 77: 85~108.
- Himmelberg G R, Loney R A. 1995. Characteristics and petrogenesis of Alaskan-type ultramafic-mafic intrusions, Southeastern Alaska. *US Geol. Surv. Prof. Pap.* 1564: 1~47.
- Hu Chaobin, Li Meng, Zha Xianfeng, Gao Xiaofeng, Li Ting. 2018. Genesis and Geological Significance of Late Paleozoic Mantle-Derived Magmatism in Qimantag, East Kunlun; A Case Study of Intrusion in Yingzhuagou. *Earth Science*, 43(12): 4334~4349 (in chinese with English abstract).
- Irvine T N. 1974. Petrology of the Duke Island ultramafic complex, southern Alaska. *Geol. Soc. Am. Memoir* 138, 240.
- Ishiwatari A, Ichiyama Y. 2004. Alaskan-type plutons and ultramafic lavas in Far East Russia, Northeast China, and Japan. *Int. Geol. Rev.* 46: 316~331.
- Jiao Jiangang, Jin Shufang, Rui Huichao, Zhang Guopeng, Ning Quanfei, Shao Leqi. 2017. Petrology, Geochemistry and Chronology Study of the Xiaokouzi Mafic-Ultramafic Intrusion in the Eastern Section of Longshou Mountains, Gansu. *Acta Geologica Sinica*, 91(4): 736~747 (in chinese with English abstract).
- Kazimoto E O, Schenk V, Berndt J. 2014. Neoproterozoic and Paleoproterozoic crust formation in the Ubendian Belt of Tanzania; Insights from zircon geochronology and geochemistry. *Precambrian Research*, 252: 119~144.
- Kazimoto E O, Schenk V, Appel P. 2015. Granulite-facies metamorphic events in the northwestern Ubendian Belt of Tanzania; Implications for the Neoproterozoic to Paleoproterozoic crustal evolution[J]. *Precambrian Research*, 256: 31~47.
- Kelemen P B, Johnson K T M, Kinzler R J, Irving A J. 1990. High-field-strength element depletions in arc basalts due to mantle-magma interaction. *Nature*, 345: 521~524.
- Ke Pezhinskas P, McDermott F, Defant M J, Hochstaedter A, Drummond M S, Hawkesworth C J, Koloskov A, Maury R C, Bellon H. 1997. Trace element and Sr-Nd-Pb isotopic constraints on a three-component model of Kamchatka Arc petrogenesis. *Geochim. Cosmochim. Acta* 61(3): 577~600.
- Kohut E J, Stern R J, Kent A J R, Nielsen R L, Bloomer S H, Leybourne M. 2006. Evidence for adiabatic decompression melting in the Southern Mariana Arc from high-Mg lavas and melt inclusions. *Contrib. Miner. Petrol.* 152(2): 201~221.
- Lawley C J M, Selby D, Condon D J, Horstwood M, Millar L, Crowley Q, Imber J. 2013. Litho geochemistry, geochronology and geodynamic setting of the Lupa Terrane, Tanzania: implications for the extent of the Archean Tanzanian Craton. *Precambrian Research*, 231: 174~193.
- Lenoir J L, Liègeois J P, Theunissen K, Klerkx J. 1994. The Palaeoproterozoic Ubendian shear belt in Tanzania: geochronology and structure. *Journal of African Earth Sciences*, 19(3): 169~184.
- Liu Fulai, Shi Jianrong, Liu Jianhui, Ye Jianguo, Liu Pingfang, Wang Fang. 2011. Protolith and ultrahigh-pressure (UHP) metamorphic ages of ultramafic rocks in Weihai area, North Sulu UHP terrane. *Acta Petrologica Sinica*, 27(4): 1075~1084 (in Chinese with English abstract).
- Liu Yongsheng, Hu Zhaochu, Gao Shan, Gunther D, Xu Juan, Gao Changhui, Cheng Hailong. 2008. In situ analysis of major and trace elements of anhydrous minerals by LA-ICP-MS without applying an internal standard. *Chemical Geology*, 257: 34~43.
- Liu Yongsheng, Hu Zhaochu, Zong Keqing, Gao Changhui, Gao

- Shan, Xu Juan, Chen Haihong. 2010. Reappraisal and refinement of zircon U-Pb isotope and trace element analyses by LA-ICP-MS. *Chinese Science Bulletin*, 55: 1535~1546.
- Loney R A, Himmelberg G R. 1992. Petrogenesis of the Pd-rich intrusion at Salt Chuck, Prince of Wales Island; an early Paleozoic Alaskan-type ultramafic body. *Canadian Mineralogist*, 30(4): 1005~1022.
- Loucks R R. 1990. Discrimination of ophiolitic from nonophiolitic ultramafic-mafic allochthons in orogenic belts by the Al/Ti ratio in clinopyroxene. *Geology*, 18(4): 346~349.
- Ludwig K R. Isoplot/Ex version 3.00. A Geochronological Toolkit for Microsoft Excel. Berkeley Geochronology Center Special Publication, 203, 4: 1~70.
- Macdonald R, Rogers N W, Fitton J G, Black S. 2001. Plume-Lithosphere Interactions in the Generation of the Basalts of the Kenya Rift, East Africa. *Journal of Petrology*, 42(5): 877~900.
- Manya S. 2011. Nd-isotope mapping of the Archean-Proterozoic boundary in southwestern Tanzania: implication for the size of the Archean Tanzanian Craton. *Gondwana Research*, 20: 325~334.
- McConnell R B. 1950. Outline of the geology of Ufipa and Ubende. Tanganyika Geological Survey: 1~62.
- Meibom A, Sleep N H, Chamberlain C P, Coleman R G, Frel R, Hren M T, Wooden J L. 2002. Re-Os isotopic evidence for long-lived heterogeneity and equilibration processes in the Earth's upper mantle. *Nature*, 419(6908): 705~708.
- Miyashiro A. 1975. Classification, characteristics, and origin of ophiolites. *Journal of Geology*, 1975, 83(2): 249~281.
- Möller A, Appel P, Mezger K, Schenk V. 1995. Evidence for a 2 Ga subduction zone; eclogites in the Usagaran belt of Tanzania. *Geology*, 23(12): 1067~1070.
- Mullen E D. 1983. MnO/TiO₂/P₂O₅: a monitor element discriminate for basalt rock/rock of oceanic environments and its implications for petrogenesis. *Earth and Planetary Science Letters*, 62: 53~62.
- Neal C R, Mahoney J J, Chazey W J. 2002. Mantle Sources and the Highly Variable Role of Continental Lithosphere in Basalt Petrogenesis of the Kerguelen Plateau and Broken Ridge LIP. Results from ODP Leg 183. *Journal of Petrology*, 43(7): 1177~1205.
- Pearce J A. 2014. Immobile element fingerprinting of ophiolites. *Elements*, 10(2): 101~108.
- Pettigrew N T, Hattori K H. 2006. The Quetico intrusions of Western Superior Province; Neo-Archean examples of Alaskan/Ural-type mafic-ultramafic intrusions. *Precambrian Research*, 149: 21~42.
- Pettigrew N T, Hattori K. The Quetico Intrusions of Western Superior Province; Neo-Archean examples of Alaskan/Ural-type mafic-ultramafic intrusions. *Precambrian Research*, 2006, 149(1): 21~42.
- Polat A, Appel P W U, Fryer B J. 2011. An overview of the geochemistry of Eoarchean to Mesoarchean ultramafic to mafic volcanic rocks, SW Greenland; Implications for mantle depletion and petrogenetic processes at subduction zones in the early Earth. *Gondwana Research*, 20(2): 255~283.
- Polat A, Fryer B, Samson M, Weisener C, Appel P W U, Frei R, Windley B F. 2012. Geochemistry of ultramafic rocks and hornblende veins in the Fiskensæset layered anorthosite complex, SW Greenland; evidence for hydrous upper mantle in the Archean. *Precambrian Research*, (214~215): 124~153.
- Qin Kezhang, Guo Zhenglin, Tang Dongmei, Li Jinxiang, Guo Xuji, Dong Lianhui. 2018. Discovery of Alaskan-type Tuerkubantao mafic-ultramafic complex in NW-Junggar, NW China and its significance. *Acta Petrologica Sinica*, 34(7): 1897~1913 (in Chinese with English abstract).
- Roberts M P, Pin C, Clemens J D, Paquette J. 2000. Petrogenesis of mafic to felsic plutonic rock associations; the Calc-alkaline Quérigut complex, French Pyrenees. *Journal of Petrology*, 2000, 41(6): 809~844.
- Sajona F G, Maury R C, Pubellier M, Leterrier J, Bellon H, Cotten J. 2000. Magmatic source enrichment by slab-derived melts in a young post-collision setting, central Mindanao (Philippines). *Lithos*, 54(3): 173~206.
- Saleeby J B. 1992. Age and tectonic setting of the Duke Island ultramafic intrusion, southeast Alaska. *Canadian Journal of Earth Sciences*, 29(3): 506~522.
- Sappin A A, Constantin M, Clark T. 2012. Petrology of mafic and ultramafic intrusions from the Portneuf-Mauricie Domain, Grenville Province, Canada; implications for plutonic complexes in a Proterozoic island arc. *Lithos* 154: 277~295.
- Shen Tingting, Zhang Lifei, Yang Jingsui, Zhang Cong, Qiu Tian, Thomas B. 2017. The characteristics and significance of age of zircon from ultramafic rocks; a case study from UHP serpentinites in Chinese southwestern Tianshan. *Acta Petrologica Sinica*, 033(012): 3783~3800 (in Chinese with English abstract).
- Su Benxun, Qin Kezhang, Sakyi P A, Malaviarachch, S P K, Liu Pingping, Tang Dongmei, Xiao Qinghua, Sun He, Ma Yuguang, Mao Qian. 2012. Occurrence of an Alaskan-type complex in the Middle Tianshan Massif, Central Asian Orogenic Belt; inferences from petrological and mineralogical studies. *Int. Geol. Rev.* 54: 249~269.
- Sun S S, McDonough W F. 1989. Chemical and isotopic systematics of oceanic basalts: implications for mantle composition and processes. *Geological Society, London, Special Publications*, 42(1): 313~345.
- Sun Hongwei, Tang Wenlong, Liu Xiaoyang, Ren Junping, Xu Kangkang, Wu Xingyuan, He Fuqing. 2018. Metallogenic Environment and Resource Potential of Orogenic Gold Deposit in Southeast Africa. *Journal of Jilin University (Earth Science Edition)*, 48(6): 1654~1668 (in Chinese with English abstract).
- Sutton J, Watson J, James T C. 1954. A study of the metamorphic rocks of Karema and Kungwe Bay, Western Tanganyika. Tanganyika Geological Survey, Bulletin 22.
- Taylor H P. 1967. The zoned ultramafic complexes of southeastern Alaska. In: Wyllie P J (Ed.), *Ultramafic and Related Rocks*. Wiley, New York: 97~121.
- Taylor S R, McLennan S M. 1985. *The continental crust: Its composition and evolution*. London: Blackwell Scientific Publications: 1~312.
- Teale E O, Eades N W, Harkin D A, Harpum J R, Horne R G. 1962. Irambo; geological map quarter degree sheet 245. Geological Survey of Tanzania, Dodoma.
- Tessalina S G, Kreshimir N, Malitch K N, Augé T, Puchkov V N, Belousova E, McInnes B A. 2016. Origin of the Nizhny Tagil clinopyroxenite-dunite Massif, Uralian Platinum Belt, Russia; insights from PGE and Os isotope systematics. *J. Petrol.* 2015: 1~21.
- Theunissen K, Lenoir J L, Liégeois J P, Delvaux D, Mruma A. 1992. Major Pan-African imprint in the Ubendian Belt of SW Tanzania; U-Pb zircon geochronology and structural context. *Comptes-rendus del Académie des Sciences de Paris* 314: 1355~1362.
- Tistl M. 1994. Geochemistry of platinum-group elements of the zoned ultramafic Alto Condoto Complex, Northwest Colombia. *Economic Geology*, 89: 158~167.
- Tulibonywa T, Manya S, Maboko M A H. 2015. Palaeoproterozoic volcanism and granitic magmatism in the Ngualla area of the Ubendian Belt, SW Tanzania; Constraints from SHRIMP U-Pb zircon ages, and Sm-Nd isotope systematics. *Precambrian Research*, 256: 120~130.
- Tulibonywa T, Manya S, Torssander P, Maboko M A. 2017. Geochemistry of the Palaeoproterozoic volcanic and associated potassic granitic rocks of the Ngualla area of the Ubendian Belt, SW Tanzania. *Journal of African Earth Sciences*, 2017, 129: 291~306.

- Turner S, Hawkesworth C, Gallagher K, Stewart K, Peate D, Mantovani M. 1996. Mantle plumes, flood basalts, and thermal models for melt generation beneath continents: Assessment of a conductive heating model and application to the Paraná. *Journal of geophysical research solid earth*, 101 (B5): 11503~11518.
- Wang K, Plank T, Walker J D, Smith E I. 2002. A mantle melting profile across the Basin and Range, SW USA. *Journal of Geophysical Research: Solid Earth*, 107(B1): 1~21.
- Wilson M. 1989. *Igneous Petrogenesis*. London: Unwin Hyman Ltd, 22.
- Wood D A. 1980. The application of a Th-Hf-Ta diagram to problems of tectonomagmatic classification and to establishing the nature of crustal contamination of basaltic lavas of the British Tertiary Volcanic Province. *Earth and Planetary Science Letters*, 50(1): 11~30.
- Woodhead J D, Hergt J M, Davidson J P, Eggins S M. 2001. Hafnium isotope evidence for 'conservative' element mobility during subduction zone processes. *Earth and Planetary Science Letters*, 192(3): 331~346.
- Worqu H, Schandelmeier H. 1996. Tectonic evolution of the Neoproterozoic Adola Belt of southern Ethiopia: evidence for a Wilson Cycle process and implications for oblique plate collision. *Precambrian Research*, 77(3~4): 179~210.
- Xu Kangkang, Liu Xiaoyang, Sun Kai, He Shengfei, Gong Penghui, Wu Xingyuan, Sun Hongwei. 2020. Zircon U-Pb LA-MC-ICP-MS Dating and Geological Significance of the Granitoids in the Ubendian Belt, Southwestern Tanzania. *Geological Survey and Research*, 43(1): 55~61 (in chinese with English abstract).
- Xu Kangkang, Liu Xiaoyang, Wang Jie, Ren Junping, Zuo Libo, He Shengfei, Wu Xingyuan, Sun Hongwei. 2019. Tectonic Evolution of the Ubendian Belt in the Southwest of Tanzania. *Geological and Exploration*, 55(2): 585~599 (in chinese with English abstract).
- Yuan Lingling, Zhang Xiaohui, Yang Zhili, Lu Yinghui, Chen Haihong. 2017. Paleoproterozoic Alaskan-type ultramafic-mafic intrusions in the Zhongtiao mountain region, North China Craton: Petrogenesis and tectonic implications. *Precambrian Research*, 296: 39~61.
- Zhang Chuanlin, Zhou Gang, Wang Hongyan, Dong Yongguan, Ding Rufu. 2010. A review on two types of mantle domains of the Permian large igneous province in Tarim and the western section of Central Asian orogenic belt. *Geological Bulletin of China*, 29(6): 779~794 (in chinese with English abstract).
- Zhang Qi, Zhang Kuiwu, Li Dazhou. 1992. *Mafic • Ultramafic Rocks in Hengduan Mountains Region*. Beijing: Science Press: 1~216 (in chinese with English abstract).
- Zhang Qi. 2014. Classifications of mafic-ultramafic rocks and their tectonic significance. *Chinese Journal of Geology*, 49(3): 982~1017 (in chinese with English abstract).
- Zhang Xiaohui, Zhang Hongfu, Tang Yanjie, Wilde S A, Hu Zhaochu. 2008. Geochemistry of Permian bimodal volcanic rocks from central Inner Mongolia, North China: Implication for tectonic setting and Phanerozoic continental growth in Central Asian Orogenic Belt. *Chemical Geology*, 249(3-4): 0~281.
- Zhou Meifu, Leshner C M, Yang Zhengxi, Li Jianwei, Sun Min. 2004. Geochemistry and petrogenesis of 270 Ma Ni-Cu-(PGE) sulfide-bearing mafic intrusions in the Huangshan district, Eastern Xinjiang, Northwest China: Implications for the tectonic evolution of the Central Asian orogenic belt. *Chemical Geology*, 209(3-4): 233~257.
- Zhou Meifu, Robinson P T, Leshner C M, Keays R R, Zhang C J, Malpas J. 2005. Geochemistry, Petrogenesis and Metallogenesis of the Panzhihua Gabbroic Layered Intrusion and Associated Fe-Ti-V Oxide Deposits, Sichuan Province, SW China. *Journal of Petrology*, 46(11): 2253~2280.
- Zuo Libo, Ren Junping, Wang Jue, Gu Alei, Sun Hongwei, Xu Kangkang, Dokowe A P, Chikambwe E. 2020. Geochemical characteristics, Zircon U-Pb ages and Lu-Hf isotopic composition of granites in Bangweulu Block, Zambia. *Geological Survey and Research*, 43(01): 30~41 (in chinese with English abstract).

参 考 文 献

- 柴凤梅, 张招崇, 董连慧, 张作衡, 吴华, 李军. 2007. 新疆中天山白石泉含铜镍矿镁铁-超镁铁岩体地球化学特征与岩石成因. *岩石学报*, 23(10): 48~60.
- 邓宇峰, 宋谢炎, 陈列猛, 程松林, 张新利, 李军. 2011. 东天山黄山西含铜镍矿镁铁-超镁铁岩体岩浆地幔源区特征研究. *岩石学报*, 27(12): 3640~3652.
- 冯延清, 钱壮志, 段俊, 孙涛, 徐刚, 姜超, 任萌, 陈宏骏. 2017. 新疆东天山铜镍成矿带西段镁铁-超镁铁质岩体成因及成矿潜力研究. *地质学报*, 91(4): 792~811.
- 何琦, 肖龙, 魏启荣, 倪平泽. 2009. 滇西吉义独蛇绿混杂岩的岩石地球化学特征、成因和构造环境探讨. *岩石学报*, 25(12): 3229~3240.
- 胡朝斌, 李猛, 查显锋, 胡朝斌, 高晓峰, 李婷. 2018. 东昆仑祁漫塔格晚古生代末期幔源岩浆活动成因及地质意义: 以鹰爪沟岩体为例. *地球科学*, 43(12): 4334~4349.
- 焦建刚, 靳树芳, 芮会超, 张国鹏, 宁权飞, 邵乐奇. 2017. 甘肃龙首山东段小口子镁铁-超镁铁质岩体岩石学、地球化学及年代学研究. *地质学报*, 91(4): 736~747.
- 刘福来, 施建荣, 刘建辉, 叶建国, 刘平华, 王舫. 2011. 北苏鲁威海地区超基性岩的原岩形成时代和超高压变质时代. *岩石学报*, 27(4): 1075~1084.
- 秦克章, 郭正林, 唐冬梅, 李金祥, 郭旭吉, 董连慧. 2018. 准噶尔西北缘吐尔库班套阿拉斯加型镁铁-超镁铁岩体的发现及意义. *岩石学报*, 2017, 34(7): 1897~1913.
- 申婷婷, 张立飞, 杨经绥, 张聪, 邱添, Thomas B. 2017. 超基性岩中锆石年龄的特征和意义——以西南天山 UHP 蛇纹岩中锆石 U-Pb 年龄为例. *岩石学报*, 033(012): 3783~3800.
- 孙宏伟, 唐文龙, 刘晓阳, 任军平, 许康康, 吴兴源, 贺福清. 2018. 非洲东南部造山型金矿成矿环境与资源潜力分析. *吉林大学学报(地球科学版)*, 48(6): 1654~1668.
- 许康康, 刘晓阳, 王杰, 任军平, 左立波, 何胜飞, 吴兴源, 孙宏伟. 2019. 坦桑尼亚西南部乌本迪带的构造演化特征. *地质与勘探*, 55(2): 585~599.
- 许康康, 刘晓阳, 孙凯, 何胜飞, 龚鹏辉, 吴兴源, 孙宏伟. 2020. 坦桑尼亚乌本迪带内花岗岩类的 LA-MC-ICP-MS 锆石 U-Pb 年龄及地质意义. *地质调查与研究*, 43(1): 55~61.
- 张传林, 周刚, 王洪燕, 董永观, 丁汝福. 2010. 塔里木和中亚造山带西段二叠纪大火成岩省的两类地幔源区. *地质通报*, 29(6): 779~794.
- 张旗, 张魁武, 李达周. 1992. 横断山区镁铁-超镁铁岩. 北京: 科学出版社. 1~216.
- 张旗. 2014. 镁铁-超镁铁岩的分类及其构造意义. *地质科学*, 49(3): 982~1017.
- 左立波, 任军平, 王杰, 古阿雷, 孙宏伟, 许康康, Alphet Phaskani Dokowe, Ezekiah Chikambwe. 2020. 赞比亚班韦乌卢地块花岗岩地球化学特征、锆石 U-Pb 年龄及 Lu-Hf 同位素组成. *地质调查与研究*, 43(01): 30~41.

Zircon U-Pb age, geochemistry and tectonic significance of the Nsamya mafic-ultramafic complex in the Ubendian Belt, southwestern Tanzania

XU Kangkang^{*1,2)}, LIU Xiaoyang^{1,2)}, SUN Kai^{1,2)}, GONG Penghui^{1,2)},
WU Xingyuan^{1,2)}, HE Shengfei^{1,2)}, SUN Hongwei^{1,2)}

1) *Tianjin Centre, China Geological Survey, Tianjin, 300170;*

2) *North China Center for Geoscience Innovation, China Geological Survey, Tianjin, 300170*

** Corresponding author; xukang06@163.com*

Abstract

The Nsamya mafic-ultramafic complex of Alaskan type was discovered for the first time in the Ubendian Belt. The study of the origin of mantle-derived magmatism is of great significance to the tectonic evolution history. The Nsamya complex has ring-shape characteristics, clinopyroxene peridotite and gabbro occur from central to northern edge. Zircon U-Pb age is between 1874Ma and 1994Ma, indicating formation in the Late Paleoproterozoic. All the rocks are characterized by low SiO₂, high MgO, FeO_T, Cr and Ni, enrichment of LREE and LILE (Ba, Pb, U), depletion of HREE and HFSE (Nb, Ta, Zr, Hf and Ti) suggesting that the Nsamya complex is the Alaskan-type formed in an arc setting. Based on the regional geological background, it is suggested that the rocks were formed during the closure of the intra-arc basin in the late stage of the Ubendian orogeny in the Paleoproterozoic, the magma came from the lithospheric mantle metasomatized by subduction fluid and experienced the crustal contamination of lower crust during underplating.

Key words: Nsamya complex; zircon U-Pb age; geochemistry; Alaskan-type; Ubendian Belt